6-11-2018

Two Results in Drawing Graphs on Surfaces

Joshua E. Fallon
Louisiana State University and Agricultural and Mechanical College, jflsu3@gmail.com

TWO RESULTS IN DRAWING GRAPHS ON SURFACES

A Dissertation

Submitted to the Graduate Faculty of the
Louisiana State University and
Agricultural and Mechanical College
in partial fulfillment of the
requirements for the degree of
Doctor of Philosophy

in

The Department of Mathematics

by
Joshua E. Fallon
B.S. in Math., Palm Beach Atlantic University, 2004
M.S., Florida Atlantic University, 2007
August 2018

Acknowledgments

This dissertation would not be possible without numerous contributions. I first thank my advisor, Professor Bogdan Oporowski, for his time, patience, and guidance. Thank you for always having a reference close to hand and for pushing me to reach for more. I have learned much more than mathematics during our time together.

Everything I have written while at LSU, especially this dissertation, is vastly improved by the tireless attention to detail given by Professor James Oxley. Thank you for going so far above and beyond the call of duty in carefully reading and thoughtfully critiquing all my written work. Thank you for the support you provided for my research and travel; you opened doors for me at every turn. I also offer my thanks to Professors Guoli Ding and Oliver Dasbach for teaching me that I can give more than my best.

The entire LSU Mathematics department has been profoundly supportive during my time here. I am especially grateful to the members of the VIGRE and GAANN committees for finding sources of funding to support my research travel. You made the difference early on between my working alone and engaging with the broader mathematics community.

It is a great pleasure to thank the community of graduate students in the department. Eric Bucher, Trey Trampel, Abiti Adili, Kim D'Souza, and Kristen Wetzler gave me a community and encouraged me when they had no idea how badly I needed it. Most of all, my academic siblings Matt, Farid, and Sarah, kept my spirits up and my eyes forward. Thank you.

This dissertation is dedicated to my wife, Gayle. Everything I do is because of you. Without your support at home I could never have started this journey, much

less finished. You have sacrificed so much for me, and I can never fully express how grateful I am.

Table of Contents

Abstract

In this work we present results on crossing-critical graphs drawn on non-planar surfaces and results on edge-hamiltonicity of graphs on the Klein bottle. We first give an infinite family of graphs that are 2-crossing-critical on the projective plane. Using this result, we construct 2-crossing-critical graphs for each non-orientable surface. Next, we use 2-amalgamations to construct 2-crossing-critical graphs for each orientable surface other than the sphere. Finally, we contribute to the pursuit of characterizing 4-connected graphs that embed on the Klein bottle and fail to be edge-hamiltonian. We show that known 4-connected counterexamples to edge-hamiltonicity on the Klein bottle are hamiltonian and their structure allows restoration of edge-hamiltonicity with only a small change.

Introduction

0.1 Basic Concepts

A *graph* is a set V of vertices and a set E of edges, where each edge connects a pair of vertices. Graphs in this document may have parallel edges but no graphs will have loops. More precisely, a graph $G = (V, E, \varphi)$ is a triple consisting of a set V of vertices, a set E of edges, and a function φ that maps each element of E to a two-element subset of V. Where there are multiple graphs under consideration, we will specify to which graph an edge set or a vertex set belongs by writing, for example, $E(G)$ for the edges of G. We refer to φ as a *incidence relation* and say e is *incident to* the elements of $\varphi(e)$. For each edge e of E, the elements of $\varphi(e)$ are the *endvertices* of e. We say two distinct edges e and f of G are *parallel edges* if $\varphi(e) = \varphi(f)$. A graph with no loops and no parallel edges is called a *simple graph*. The number of edges incident to a vertex v is the *degree* of v. For an integer $k \geq 0$, a *k-separation* of G is an unordered pair $\{G_1, G_2\}$ of proper induced subgraphs of G such that $G_1 \cup G_2 = G$ and $|V(G_1 \cap G_2)| = k$. A graph on more than k vertices is *k-connected* if for each non-negative $k' < k$ the graph has no k'-separation.

There are numerous ways we may discuss a containment relationship between two graphs. We include here the three we will use in this work. If a graph H can be obtained from another graph G by deleting vertices and edges then H is a *subgraph* of G. To *subdivide* an edge of H, replace the edge with a path. If H' is obtained by subdividing some subset of $E(H)$, then H' is a *subdivision* of H. If G has a subgraph isomorphic to a subdivision of H, then H is a *topological minor* of G. To *contract* an edge e of G with endvertices u and v, delete e and identify u and v; we denote the resulting graph G/e. This operation may create some loops; since we do not permit loops, we shall always delete loops created by contraction of an edge.

If H can be obtained from G by a sequence of edge deletions, edge contractions, and deletions of degree-zero vertices, carried out one at a time in any order, then H is a *minor* of G.

The main results of this work involve drawings and embeddings of graphs in surfaces. A *surface* is a compact Hausdorff space that is locally homeomorphic to the unit disk in $\mathbb{R}^2$. To add a *crosscap* to a surface Σ, remove the interior of a disk in Σ and identify the the members of each diametrically opposed pair of points on the boundary of the disk. A surface with $n \geq 1$ crosscaps is a *non-orientable surface of genus* n, written $\mathbb{N}_n$. To add a *handle* to a sphere, remove the interiors of two disks and identify the boundary cycles with opposing orientations. A surface with $k \geq 0$ handles is an *orientable surface of genus* k, written $\mathbb{S}_k$. The classification theorem of closed surfaces is a well-known result in topology. It states that each surface is homeomorphic to the sphere or the sphere with a finite number k of handles added or the sphere with a finite number n of crosscaps added. The *Euler characteristic* of a surface Σ is given by $\varepsilon(\Sigma) = 2 - 2k$ if Σ is orientable or $\varepsilon(\Sigma) = 2 - n$ if Σ is non-orientable.

We review here some basic ideas of embedding graphs in surfaces. For a more comprehensive treatment of graphs on surfaces, we refer the reader to [20]. An *embedding* of a graph G in a surface Σ is a map $\Gamma : G \to \Sigma$ that maps each vertex of G to a point of Σ and each edge of G to a simple arc (homeomorphic image of $[0, 1]$) in Σ, subject to the following constraints:

- No two vertices are mapped to the same point.
- If an edge e of G is incident to a vertex v, then $\Gamma(v)$ is an endpoint of the arc $\Gamma(e)$.

- If e and f are distinct edges of G, then $\Gamma(e) \cap \Gamma(f)$ is the image under Γ of the set of vertices incident to both e and f.

A *good drawing* of G on Σ is a map Γ that maps vertices of G to points of Σ and edges of G to simple arcs in Σ, subject to the following constraints:

- No two vertices are mapped to the same point.
- If an edge e of G is incident to a vertex v, then $\Gamma(v)$ is an endpoint of $\Gamma(e)$.
- If e and f are distinct edges of G and v is an endvertex of both edges, then $\Gamma(v) \in \Gamma(e) \cap \Gamma(f)$; if there is no such vertex, $\Gamma(e) \cap \Gamma(f)$ consists of at most one point interior to both arcs.
- If e, f, and h are distinct edges of G such that no vertex is incident to all three, then $\Gamma(e) \cap \Gamma(f) \cap \Gamma(h) = \varnothing$.

All drawings considered in this dissertation will be good drawings, so no drawing will contain one of the configurations shown in Figure 1.

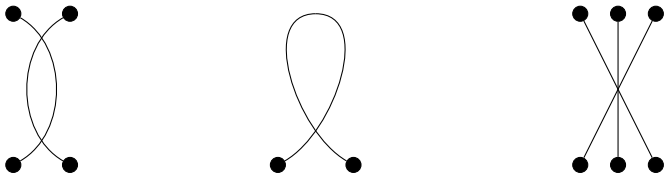

Figure 1. Configurations prohibited in a good drawing.

A reader desiring precise definition of terms not defined here may consult a textbook on graph theory, such as [7]. Terminology and notation used in this document without explicit definition is standard and unambiguous in the graph theory literature.

0.2 Graph Embeddings and Crossing Numbers

If a graph G has an embedding in a surface Γ, we say G is *embeddable* in Σ. For each of the surface $\mathbb{S}_0$ (the sphere) and $\mathbb{N}_1$ (the projective plane), a structural result characterizes the graphs embeddable in that surface.

Theorem 0.1 (Kuratowski)**.** *A graph G is embeddable in the sphere if and only if G has no subgraph isomorphic to a subdivision of at least one of $K_{3,3}$ or K_5.*

Kuratowski's theorem leads to a characterization of planar graphs in terms of forbidden minors as well as forbidden topological minors, and the set of minimal obstructions is the same for both containment relations. Archdeacon's result implies a list of 35 minor-minimal obstructions to embeddability in the projective plane.

Theorem 0.2 (Archdeacon)**.** *A graph G is embeddable in the projective plane if and only if G has no topological minor isomorphic to a member of a list of 103 specified graphs.*

One result of the much-celebrated Graph Minors Project implies that for each surface the list of subgraphs (up to subdivision) whose presence prevents embeddability in that surface is finite. The above results are the only explicit characterizations of forbidden topological minors for embeddability in a surface; the length of the list seems to grow very quickly with the genus of the surface considered. For the torus, there are currently $250,815$ forbidden topological minors and 17,523 forbidden minors known [22]. While a forbidden-subgraph characterization of embeddability in a fixed surface exists for only the sphere and the projective plane, Mohar describes in [19] an algorithm for determining whether a given graph embeds in a surface of fixed (orientable or non-orientable) genus that is linear in the graph size and doubly exponential in the graph genus. If a graph G embeds in $\mathbb{S}_k$

but not in $\mathbb{S}_{k+1}$, we say the *orientable genus* of G is k. Similarly, if G embeds in $\mathbb{N}_n$ but not in $\mathbb{N}_{n+1}$, we say the *non-orientable genus* of G is n. Thomassen shows in [34] that, given a graph G and a natural number k, the problem of determining whether G has genus (orientable or non-orientable) at most k is NP-complete.

If G cannot be embedded in a surface Σ of genus k, then each good drawing of G on Σ must have at least one *crossing*. A crossing in a drawing $\Gamma(G)$ on Σ is a point that is in $[\Gamma(e) \cap \Gamma(f)] \setminus \Gamma(V)$ for some distinct edges e and f of G. If $\Gamma(G)$ has exactly t crossings for some positive integer t, then Γ is a *t-drawing* of G on Σ. A drawing with no crossings is an *embedding*. If G has a t-drawing on Σ but no s-drawing for $s < t$, then G has *crossing number* t on Σ, written $\mathrm{cr}_\Sigma(G) = t$. Our first main result, addressed in Chapters 1 and 2, is on *crossing-critical* graphs. If G has crossing number at least t on Σ, but $\mathrm{cr}_\Sigma(H) < t$ for all proper subgraphs H of G, then we say G is *t-crossing-critical* on Σ. We may consider the results of Theorems 0.1 and 0.2 as characterizations of the 1-crossing-critical graphs on the sphere and projective plane. It is not true in general that a k-crossing-critical graph on Σ has crossing number k; consider a large complete graph K_n. Deletion of an edge decreases the crossing number on Σ by the order of n^2, so K_n is t-crossing-critical for many values of t. Implicit in identifying a graph as k-crossing-critical is determining whether, given a graph and integer k, the graph's crossing number is at least k; this question is shown in [9] to be NP-complete.

0.3 Hamiltonicity

Our second main result is on hamiltonicity of graphs embedded in surfaces. A graph is *hamiltonian* if it contains a cycle that includes all vertices; such a cycle is a *hamilton cycle*. If a graph contains for each edge a hamilton cycle that includes that edge, we say the graph is *edge-hamiltonian*. Karp shows in [17] that the problem of determining whether an arbitrary graph has a hamilton cycle is NP-complete.

Since then, much work has been done in identifying structural properties of graphs that imply hamiltonicity. For an overview of questions in hamiltonicity, we refer the reader to Gould's series of surveys [11], [12], [13] and Kawarabayashi's survey [18]. We are concerned primarily with a conjecture of Nash-Williams in [24] that every 4-connected graph embeddable in the Klein bottle is hamiltonian. In [32] and [29], 4-connected graphs that embed in the plane and projective plane, respectively, are shown to be edge-hamiltonian, a stronger condition than hamiltonicity. Among graphs that embed in the torus or the Klein bottle, there are 4-connected graphs that are not edge-hamiltonian. We contribute to a characterization of those 4-connected Klein-bottle graphs that are not edge-hamiltonian, and observe that known counterexamples to edge-hamiltonicity are nonetheless hamiltonian graphs. In particular, we show that known counterexamples to edge-hamiltonicity on the Klein bottle are *critical* in a sense different from that of crossing-critical graphs. These graphs are critical with respect to non-edge-hamiltonicity in that addition of a certain type of edge restores edge-hamiltonicity.

After presenting these two results, we consider in Chapter 7 some directions for extending this work. Our results on 2-crossing-critical graphs on orientable surfaces suggest a relationship between additivity of crossing number and additivity of genus for amalgamations of graphs. With this in mind, we suggest an approach to constructing 2-connected 2-crossing-critical graphs on surfaces of fixed genus by joining 2-crossing-critical graphs on surfaces of lower genus. Our demonstration of the criticality of counterexamples to edge-hamiltonicity on the Klein bottle is not complete; in the conclusion we consider how to approach the unresolved cases and counterexamples that arise differently.

Chapter 1
Crossing-Critical Graphs

In this chapter we survey some results on 1- and 2-crossing-critical graphs for the plane and the projective plane. Since our main result on 2-crossing-critical graphs uses so-called *tile belts*, we introduce tile graphs and present some important properties of tiles that are essential to understanding tile belts. The discussion in this chapter presents the tools we will use in Chapter 2 to achieve our primary result.

1.1 Preliminaries

The 1-crossing-critical graphs are given for the plane and projective plane by Kuratowski and Archdeacon, respectively. For both orientable and non-orientable surfaces of higher genus, the list of 1-crossing-critical graphs is still unknown. A nearly complete characterization of 2-crossing-critical graphs for the plane is given by Bokal, Oporowski, Richter, and Salazar [2]; their characterization capitalizes on the structure of graphs that have a topological minor isomorphic to V_{10}, the Möbius ladder on 10 vertices, or do not have a topological minor isomorphic to V_8. Of particular interest in their characterization are the 3-connected graphs with a V_{10} topological minor; these are members of a family of twisted tile belts.

For the plane, tiles have contributed a great deal toward understanding crossing-critical graphs. After the initial development of tile study by Pinontoan and Richter [25, 26], Bokal [1] used tiles to generate infinite families of crossing-critical graphs on the plane. Richter's work illustrates the strength of the structure imposed by tiles, as his work allows prescription of average degree and crossing number. Essential to Bokal's work is the ease with which crossing number can be determined in large tiled graphs, and this sparked interest in determining how far crossing-critical

graphs can be from tiled graphs. The authors of [2] show that large 2-crossing-critical graphs have structure described by tiles.

For the projective plane, Hliněný and Salazar [16] use tiles to construct an infinite family of 2-crossing-critical graphs with a vertex of arbitrarily high degree showing that, unlike the plane, there are 2-crossing-critical graphs on the projective plane with unbounded bandwidth. The *bandwidth* of a graph is the minimum value of $\max\{|f(u) - f(v)| : uv \in E\}$ taken over all labelings f that map each vertex to a distinct integer. In the next chapter, we present a family of 3-connected graphs that are 2-crossing-critical on the projective plane and have bounded bandwidth. These graphs are adapted from the 3-connected graphs that contain a V_{10} minor and are 2-crossing-critical on the plane, giving some insight into how the tile structure of 2-crossing-critical graphs on the plane allows extension to surfaces of higher genus. This work binds together the results of [2] and [16], showing that a high-degree vertex is not essential to adapting a tile belt to a 2-crossing-critical graph on the projective plane and that there is a natural technique for adapting certain crossing-critical graphs from the plane to the projective plane.

1.2 Tiles

Since our result centers on graphs constructed using tiles, and in particular some results on such graphs in the case of drawings on the plane, we include the following definitions from [2].

Definition 1.1.

1. *A* tile *is a triple $T = (G, \lambda, \rho)$ consisting of a graph G and two sequences λ and ρ of distinct vertices of G, with no vertex of G appearing in both λ and ρ.*

2. *A* tile drawing *is a drawing* Γ *of* G *in the unit square* $[0,1] \times [0,1]$ *for which the intersection of the boundary of the square with* $\Gamma(G)$ *contains precisely the images of the vertices of the* left wall λ *and the* right wall ρ*, and these are drawn in* $\{0\} \times [0,1]$ *and* $\{1\} \times [0,1]$*, respectively, such that the* y*-coordinates of the vertices are in increasing order with respect to their orders in the sequences* λ *and* ρ*.*

3. *The* tile crossing number $\mathrm{tcr}(T)$ *of a tile* T *is the smallest number of crossings in a tile drawing of* T*.*

4. *A tile* T *is planar if* $\mathrm{tcr}(T) = 0$*.*

5. *A* k-tile-drawing *of a tile is a tile drawing with at most* k *crossings.*

Since we are constructing a family of graphs by adhering small tiles to create a large tile, we formalize this notion as follows.

Definition 1.2.

1. *The tiles* $T = (G, \lambda, \rho)$ *and* $T' = (G', \lambda', \rho')$ *are* compatible *if* $|\rho| = |\lambda'|$*.*

2. *A sequence* $(T_0, T_1, \ldots, T_m)$ *of tiles is* compatible *if, for each* $i = 1, 2, \ldots, m$*, the tiles* T_{i-1} *and* T_i *are compatible.*

3. *The* join *of compatible tiles* (G, λ, ρ) *and* (G', λ', ρ') *is the tile* $(G, \lambda, \rho) \otimes (G', \lambda', \rho')$ *whose graph is obtained from* G *and* G' *by identifying the sequence* ρ *term by term with the sequence* λ'*; the left wall is* λ *and the right wall is* ρ'*.*

4. *As* $\otimes$ *is associative, the join* $\otimes\mathcal{T}$ *of a compatible sequence* $\mathcal{T} = (T_0, T_1, \ldots, T_m)$ *of tiles is well-defined as* $T_0 \otimes T_1 \otimes \cdots \otimes T_m$*.*

The following two definitions from [2] provide us with precise language to describe the construction of the graphs of interest from tiles and to discuss crossing-criticality.

Definition 1.3.

1. *A tile T is* cyclically compatible *if T is compatible with itself.*

2. *For a cyclically-compatible tile T, the* cyclization *of T is the graph $\circ T$ obtained by identifying the respective vertices of the left wall with the right wall. A cyclization of a cyclically-compatible sequence $\mathcal{T}$ of tiles is defined as $\circ\mathcal{T} = \circ(\otimes\mathcal{T})$.*

Definition 1.4.

1. *For a sequence ω, the reversed sequence is denoted $\overline{\omega}$.*

2. - *The* right-inverted *tile of a tile $T = (G, \lambda, \rho)$ is the tile $T^{\updownarrow} = (G, \lambda, \overline{\rho})$;*
   - *the* left-inverted *tile is ${}^{\updownarrow}T = (G, \overline{\lambda}, \rho)$;*
   - *the* inverted *tile is ${}^{\updownarrow}T^{\updownarrow} = (G, \overline{\lambda}, \overline{\rho})$.*

3. *A tile T is* k-degenerate *if T is planar and, for every edge e of T,* $\mathrm{tcr}(T^{\updownarrow}\backslash e) < k$.

With these definitions in hand, we make the following useful observations about tiles and their joins.

Observation 1.5. *The tile crossing numbers of a tile T and its inversion ${}^{\updownarrow}T^{\updownarrow}$ are equal.*

A tile drawing of ${}^{\updownarrow}T^{\updownarrow}$ can be obtained from a tile drawing of T, maintaining the number of crossings in the tile drawing, by the automorphism $(x, y) \mapsto (x, 1 - y)$ of the unit square.

Observation 1.6. *Let $(T_0, T_1, \ldots, T_m)$ be a compatible sequence $\mathcal{T}$ of tiles. Then*

$$\operatorname{tcr}(\otimes\mathcal{T}) \leq \sum_{i=0}^{m} \operatorname{tcr}(T_i).$$

For $i = 0, 1, \ldots, m$, suppose $\lambda_i = [\lambda_{i,1}, \lambda_{i,2}, \ldots, \lambda_{i,|\lambda_i|}]$ and $\rho_i = [\rho_{i,1}, \rho_{i,2}, \ldots, \rho_{i,|\rho_i|}]$. For each i, draw T_i in the unit square $[i, i+1] \times [0, 1]$ with $\lambda_{i,j}$ at $(i, \frac{1}{|\lambda_i|})$ and $\rho_{i,j}$ at $(i+1, \frac{1}{|\rho_i|})$. The resulting drawing is a drawing $\Gamma(\otimes\mathcal{T})$ in $[0, m+1] \times [0, 1]$, and the horizontal contraction of Γ that maps (x, y) to $(\frac{x}{m+1}, y)$ is a tile drawing with $\sum_{i=0}^{m} \operatorname{tcr}(T_i)$ crossings.

Since our graphs of immediate interest are constructed from the cyclization of a sequence of compatible tiles, the following observation on cyclization of a tile is quite useful.

Observation 1.7. *Let T be a cyclically compatible tile. Then* $\operatorname{cr}(\circ T) \leq \operatorname{tcr}(T)$.

If a tile T is cyclically compatible, then it may be drawn in the unit square with $\operatorname{tcr}(T)$ crossings and the i^{th} elements of the sequences λ and ρ having the same y-coordinate for each i. Identification of the right and left boundaries of the unit square as in the standard planar representation of a cylinder thus gives a $\operatorname{tcr}(T)$-drawing of $\circ T$ on the cylinder, which is a restriction of the sphere.

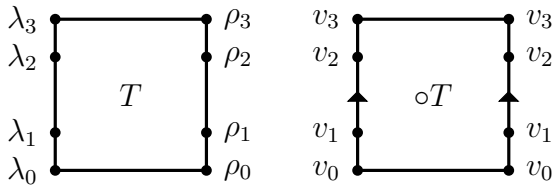

Figure 1.1. Identification of the left and right boundaries of the unit square gives a drawing on a cylinder.

Our extension from a set of base cases to an infinite family of 2-crossing-critical graphs on the projective plane relies heavily on the following lemma from [2].

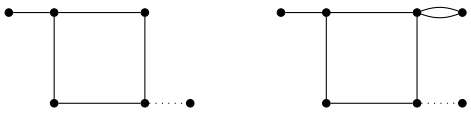

Figure 1.2. The two frames.

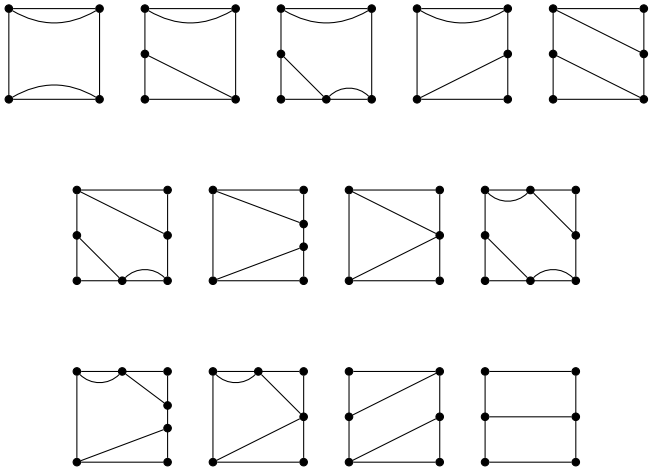

Figure 1.3. The thirteen pictures.

Lemma 1.8. *Let $\mathcal{T} = (T_0, \ldots, T_m)$ be a sequence of k-degenerate tiles. Then $\otimes(\mathcal{T})$ is a k-degenerate tile.*

Proof. By Observation 1.6, we know $\otimes(\mathcal{T})$ is planar. Let e be an edge of $\otimes\mathcal{T}$ and T_i the tile of $\mathcal{T}$ containing e. Let $\mathcal{T}' = (T_0, \ldots, T_{i-1}, T_i^{\updownarrow}\backslash e, {}^{\updownarrow}T_{i+1}^{\updownarrow}, \ldots, {}^{\updownarrow}T_m^{\updownarrow})$, so $\otimes\mathcal{T}' = \otimes\mathcal{T}^{\updownarrow}\backslash e$; in particular, $\mathrm{tcr}(\otimes\mathcal{T}') = \mathrm{tcr}(\otimes\mathcal{T}^{\updownarrow}\backslash e)$. The k-degeneracy of each T_i implies $\mathrm{tcr}(T_i^{\updownarrow}\backslash e) < k$. Since all other tiles of $\mathcal{T}'$ are planar, Observation 1.6 implies $\mathrm{tcr}(\otimes\mathcal{T}^{\updownarrow}\backslash e) \leq \mathrm{tcr}(T_i^{\updownarrow}\backslash e) < k$. □

Let $\mathcal{S}$ be the set of tiles obtained by filling one of the two *frames* shown in Figure 1.2 with one of the *pictures* shown in Figure 1.3 by identifying the two squares, as defined in [2]. Each picture may be inserted into a frame as shown or rotated 180°. We remark that since all tiles in use have frames as shown in Figure 1.2 and λ and ρ are given as the left and right vertex sets of the frame for each tile, regardless of the picture inside, each pair of tiles in $\mathcal{S}$ is compatible.

1.3 The Plane

In [2], a nearly complete characterization of 2-crossing-critical graphs is given for the plane. In particular, the authors characterize the following:

1. 3-connected, 2-crossing-critical graphs without a V_8 topological minor
2. 3-connected, 2-crossing-critical graphs with a V_{10} topological minor
3. 2-crossing-critical graphs of connectivity at most two (obtained from 3-connected 2-crossing-critical graphs)

The remaining graphs with a V_8 topological minor but no V_{10} topological minor are shown to have at most three million vertices. A construction is given for the 3-connected 2-crossing-critical graphs with no V_8 topological minor.

The set $\mathcal{T}(\mathcal{S})$ of graphs we adapt for the projective plane contains all 3-connected, 2-crossing-critical graphs with a V_{10} topological minor. We include the definition of $\mathcal{T}(\mathcal{S})$ from [2] below.

Definition 1.9. *The set $\mathcal{T}(\mathcal{S})$ consists of all graphs of the form $\circ\left((\otimes\mathcal{T})^{\updownarrow}\right)$, where $\mathcal{T}$ is a sequence $\left(T_0, {}^{\updownarrow}T_1^{\updownarrow}, T_2, \ldots, {}^{\updownarrow}T_{2m-1}^{\updownarrow}, T_{2m}\right)$ such that $m \geq 1$ and for i from 0 to $2m$ each tile T_i is in $\mathcal{S}$.*

We make two remarks about the set $\mathcal{T}(\mathcal{S})$. First, if two consecutive tiles in $\mathcal{T}$ have degree-one vertices identified by a join, we suppress the resulting degree-two vertex. Second, while not every graph in $\mathcal{T}(\mathcal{S})$ has a V_{10} topological minor, all 3-connected, 2-crossing-critical graphs with a V_{10} topological minor are in this set.

Since we will refer to this result throughout the next chapter, we include here Theorem 2.18 of [2].

Theorem 1.10. *If $G \in \mathcal{T}(\mathcal{S})$, then G is 2-crossing-critical on the plane.*

The *rim* of an element of $\mathcal{T}(\mathcal{S})$ is the cycle R that consists of the top and bottom horizontal path in each frame (including the part that sticks out in either side) and, if there is a parallel pair in the frame, one of the two edges of the parallel pair. If we do not give the last tile a half-twist on the right before identifying the right boundary of T_{2m} with the left boundary of T_0, then the top horizontal paths in each frame form a cycle R_1 that is disjoint from the cycle R_2 formed by the bottom horizontal paths in each frame, giving the graph a broad structure more like a circular ladder than a Möbius ladder. In the next chapter we will consider tile belts that are not twisted, as drawing a circular ladder through the crosscap of the projective plane introduces a twist in one of the tiles. The main result of the next chapter capitalizes on that behavior.

Chapter 2
2-Crossing-Critical Graphs on the Projective Plane

In this chapter we define a set of graphs that are 2-crossing-critical on the projective plane. We give a construction for these graphs, which are composed of tiles, and use properties of tile graphs to show both the crossing number and its criticality for each graph in the set.

2.1 From the Plane to the Projective Plane

Graphs in the set $\mathcal{T}(\mathcal{S})$, defined in Chapter 1, that contains all 3-connected, 2-crossing-critical graphs for the plane with a V_{10} topological minor, have an overarching structure similar to a Möbius ladder. A set of untwisted tile belts that are 2-crossing-critical on the projective plane is given in [16]; the crossings are forced by the addition of a vertex that is adjacent to three vertices on each tile. The following construction is given in [16].

Let T denote the tile graph on 11 vertices and 15 edges depicted in Figure 2.1 in solid lines, with left boundary vertices a and b and right boundary vertices d and c. Denote by T^2 the graph $T \otimes {}^{\updownarrow}T^{\updownarrow}$, where the copies of named vertices of T are indicated with apostrophes in ${}^{\updownarrow}T^{\updownarrow}$ (with dashed edges in Figure 2.1), so c is identified with a' and d with b'.

Let $T_0^2, \ldots, T_{t-1}^2$ be t disjoint copies of the graph T^2, where the boundary vertices of T_i^2 are labeled a_i, b_i, c_i', and d_i'. For $0 \leq i \leq t-1$ identify c_i with a_{i+1} (where

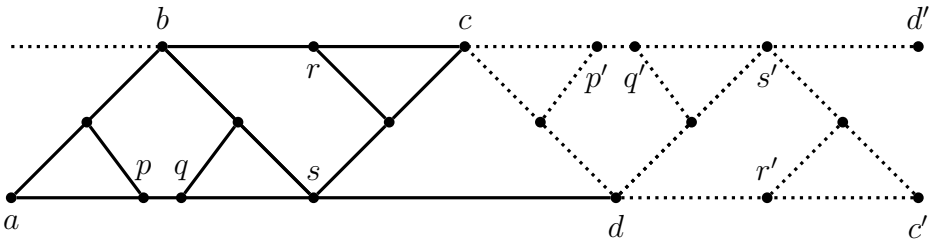

Figure 2.1. One tile T used in the construction of H_t (in solid lines); and another attached copy of ${}^{\updownarrow}T^{\updownarrow}$ (a scheme in dashed lines), together forming T^2.

all indices are taken modulo t) and identify b_i with d_{i+1}. Denote the resulting graph by H'_t and observe that, unlike graphs in $\mathcal{T}(\mathcal{S})$, the graph H'_t is planar. Denote by p_i, q_i, r_i and p'_i, q'_i, r'_i the copies of the vertices p, q, and r in each T^2_i. Finally, let H_t be the graph obtained by adding a new vertex h to H'_t and edges $hp_i, hq_i, hr_i, hp'_i, hq'_i, hr'_i$ for each i from 0 to $t-1$. We can now state Theorem 1.4 of [16].

Theorem 2.1. *There is an infinite family of simple 3-connected graphs H_t, $t \geq 4$, such that each H_t is 2-crossing-critical in the projective plane and has a vertex of degree $6t$.*

We make a few observations about the graphs H_t. First, these graphs have unbounded bandwidth. Richter and Salazar conjecture [27] that for each integer $k > 0$ there is a number $B(k)$ such that all k-crossing-critical graphs have bandwidth at most $B(k)$. While this may still be true for the plane, the graphs H_t are counterexamples for 2-crossing-critical graphs on the projective plane. Second, these graphs are simple. Many crossing-critical graphs can be obtained from replacing sets of edges in simple graphs with parallel classes. For example, replacing each edge of a Kuratowski graph with a parallel class of size k creates a k^2-crossing-critical graph. Finally, a graph H'_t cannot be adapted simply to a 2-crossing-critical graph for the plane by replacing some T^2_i with $(T^2_i)^{\updownarrow}$ or $T^{\updownarrow}_i$ and deleting the high-degree vertex. Such a graph has a V_{10} topological minor (as does H_t), but is not in the set $\mathcal{T}(\mathcal{S})$.

We introduce here an infinite set of graphs that have bounded bandwidth, include both simple graphs and graphs with parallel edges, and are adapted from the 2-crossing-critical graphs for the plane. Using the set $\mathcal{S}$ of tiles defined in Chapter 1, we define $\mathcal{T}'(\mathcal{S})$ to be all graphs of the form $\circ(\otimes\mathcal{T})$, where $\mathcal{T}$ is a sequence $\left(T_0, {}^{\updownarrow}T^{\updownarrow}_1, T_2, \ldots, T_{2m}, {}^{\updownarrow}T^{\updownarrow}_{2m+1}\right)$ of tiles in $\mathcal{S}$ for $m \geq 2$. Note that graphs in $\mathcal{T}'(\mathcal{S})$

are planar, and can be obtained from graphs in $\mathcal{T}(\mathcal{S})$ by replacing the last tile $T_{2m}^{\updownarrow}$ with a join of tiles $T_{2m} \otimes^{\updownarrow} T_{2m+1}^{\updownarrow}$. For each i, let v_i be the frame vertex incident to the right dotted edge in Figure 1.2 that is identified with a vertex of the picture inside T_i. We define the family $\mathcal{T}_a^+(\mathcal{S})$ to be the graphs obtained by adding to each member of $\mathcal{T}'(\mathcal{S})$ a new vertex v adjacent to v_i for each of three odd indices and each of three even indices i with indices alternating parity as they increase.

It is easy to see that graphs in $\mathcal{T}_a^+(\mathcal{S})$ can be 2-drawn on the projective plane, as shown in the small example G in Figure 2.2, where points on opposite sides of the ellipse are identified:

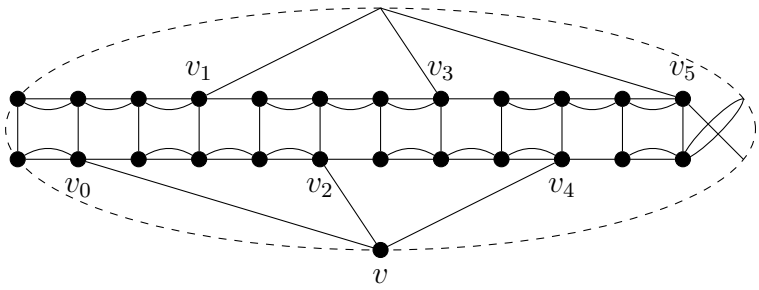

Figure 2.2. A 2-drawing of a small example.

This example illustrates how we may apply Lemma 2.11 of [2] to show $\mathrm{cr}(G\backslash e) < 2$ for each edge e of G not incident to v. Removal of an edge from a tile T leaves a tile with twisted tile crossing number less than 2. The only remaining edges whose removal we need to verify decreases the crossing number below 2 are edges incident with v. Since we can perturb a drawing of G along the tile belt and can flip all the tiles and obtain another graph in $\mathcal{T}(\mathcal{S})$ we see that, for the purposes of deletion to reduce crossing number, all edges incident to v are interchangeable. We give a drawing of $G\backslash vv_3$ in Figure 2.3 to illustrate $\mathrm{cr}(G\backslash e) < 2$ for all remaining choices of e.

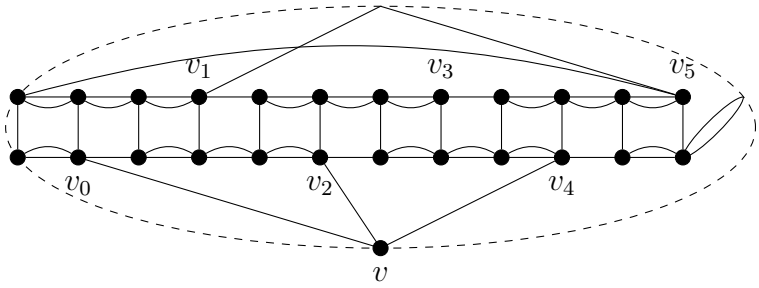

Figure 2.3. The second case of crossing number less than 2.

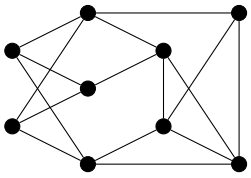

Figure 2.4. $F1$, an obstruction to embeddability in the projective plane.

2.2 A Partial Embedding

For crossing-critical graphs composed of tiles, proving the criticality of the crossing number can be more difficult than determining the crossing number itself, as this requires determining the crossing number of $G \backslash e$ for each edge e of G. In this section we prove the following key lemma, establishing the crossing number of graphs in $\mathcal{T}_a^+(\mathcal{S})$.

Lemma 2.2. *The graphs in $\mathcal{T}_a^+(\mathcal{S})$ have crossing number two on the projective plane.*

We first observe that the projective crossing number of each graph in $\mathcal{T}_a^+(\mathcal{S})$ is at least one. To see this, consider a *framework* F obtained from a graph in $\mathcal{T}_a^+(\mathcal{S})$ by replacing the picture in each tile with a four-cycle. This graph has a topological minor isomorphic to $F1$, a forbidden graph for projective plane embedding, so every drawing of the framework in the projective plane has at least one crossing.

We employ a constructive test for embeddability in the projective plane to determine pairs of edges of the framework that must cross. In particular, we focus on

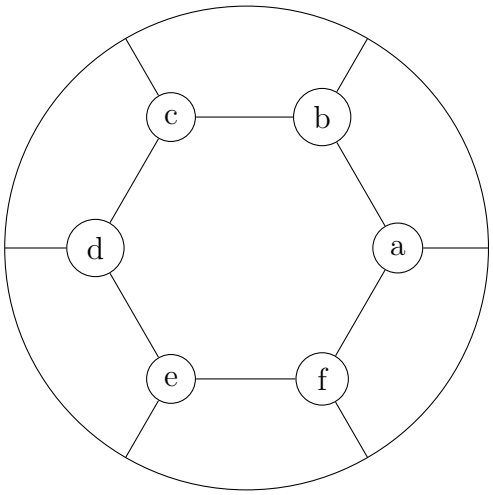

Figure 2.5. One labeling of an embedding of $K_{3,3}$ in the projective plane.

a subgraph of F isomorphic to a subdivision of $K_{3,3}$, to which we shall refer as $\mathcal{U}$. Since F has a $\mathcal{U}$ subgraph, we first consider all embeddings of this subgraph in the projective plane. To follow the algorithm described in [21] that returns either an embedding of a graph in the projective plane or a subgraph with crossing number at least one, we make use of the following theorem from [20].

Theorem 2.3. *There is only one unlabeled embedding of $K_{3,3}$ in the projective plane and there are six non-equivalent ways to label this embedding (by permutations of one color class), as shown in Figure 2.5.*

We specify in F the branch vertices of $\mathcal{U}$ in Figure 2.6 and show five prohibited embeddings in Figure 2.7. The embeddings that lead to drawings with few crossings on the projective plane are determined by the $\mathcal{U}$-bridges of F, where bridges are defined as follows. For a subgraph H of G, an H-bridge is a subgraph of G that is either an edge not in H both of whose endvertices are in H or the union of a connected component of $G\backslash H$ with all edges that have one vertex in the component and one vertex in H and the endvertex in H of each of these edges. The vertices shared by an H-bridge and H are the *attachment points* of the bridge.

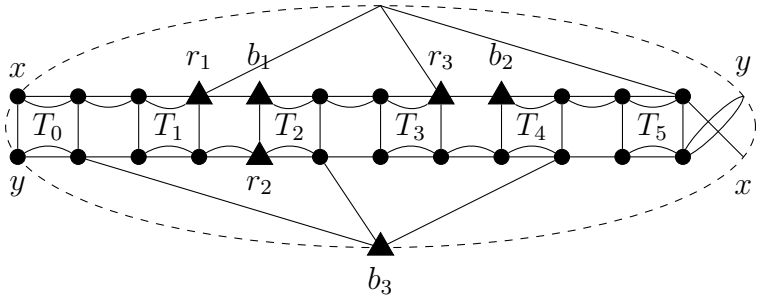

Figure 2.6. The branch vertices of a $\mathcal{U}$ subgraph are labeled by color class.

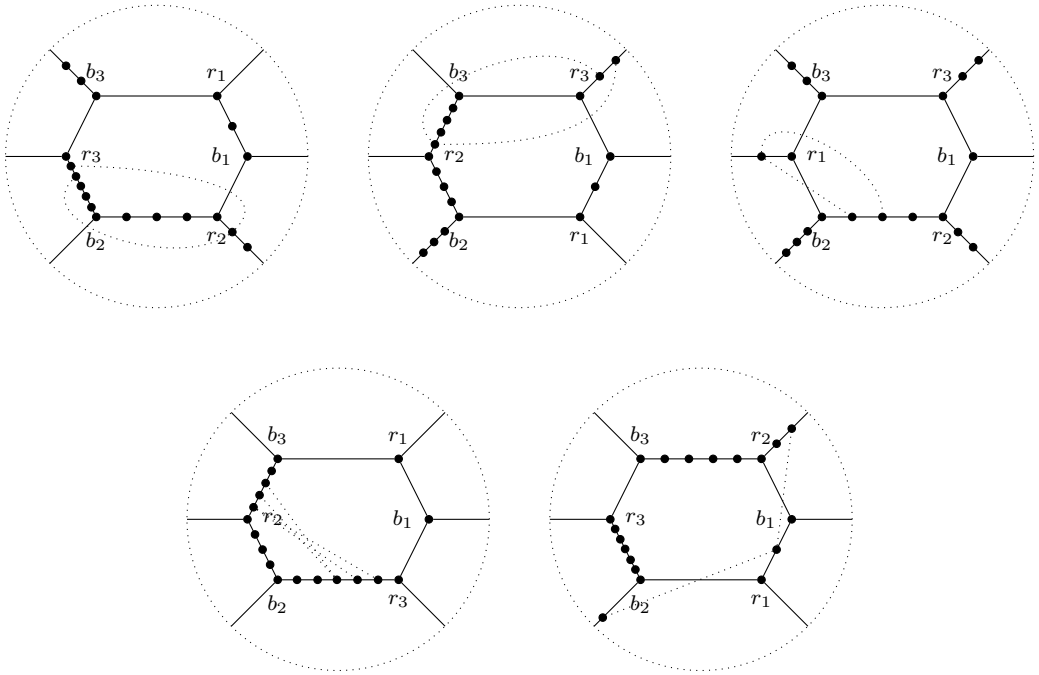

Figure 2.7. $\mathcal{U}$-bridges in five of the six embeddings of $\mathcal{U}$ lead to at least two crossings in an empty framework.

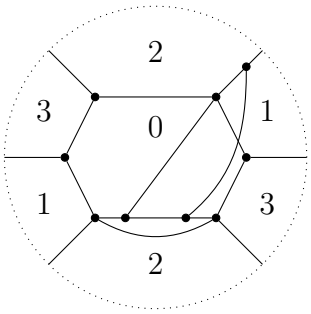

Figure 2.8. An F1-minor of F with regions of $K_{3,3}$ labeled.

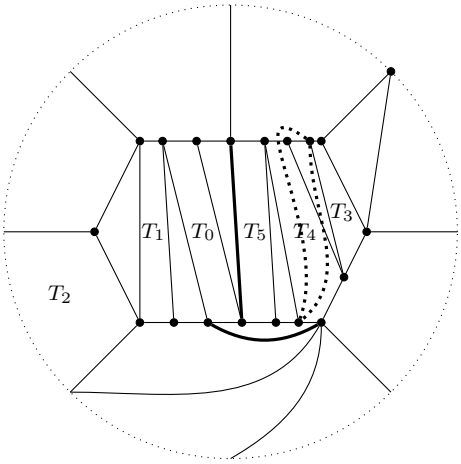

Figure 2.9. A 1-drawing of F.

Because the addition of pictures to the frames in each tile adds some crossings, we see that we may restrict our focus to a particular tile. The symmetry of the framework implies we need not specify which tile we consider.

There is only one permutation of the branch vertices of a $\mathcal{U}$ subgraph of F that permits a 1-drawing of the framework on the projective plane; in this drawing the remaining edges of F restrict assignment of the edges of F1 to faces of $\mathcal{U}$ as shown in Figure 2.9. The thick edges are $\mathcal{U}$-bridges of the F1 minor (note this includes the thick dotted edge), and the dotted edge can cross in either of the two places shown; only one of the two arcs shown corresponds to an edge of F.

We focus now on the picture filling the tile T_4. Figure 2.2 shows that if the tile crossing number of $T_i^{\updownarrow}$ is less than 2 for some i, the graph G obtained from F by filling in T_i has crossing number 1 on the projective plane. It follows that

Figure 2.10. Tile drawings of T_4, $T_4^{\updownarrow}$, and ${}^{\updownarrow}T_4$.

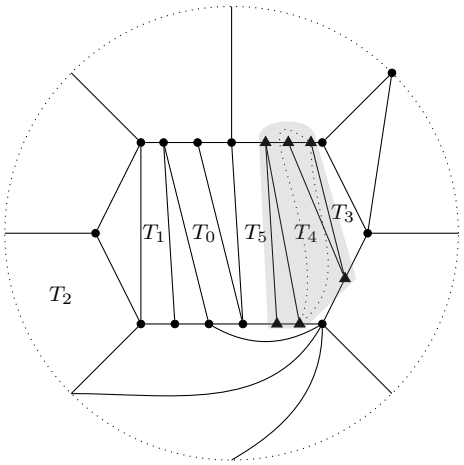

Figure 2.11. A 1-drawing of F with a disk D containing T_4 highlighted.

$\operatorname{tcr}\left(T_i^{\updownarrow}\right) \geq 2$. Consider the frame of T_4 and the frames of $T_4^{\updownarrow}$ and ${}^{\updownarrow}T_4$ shown in Figure 2.10. The symmetry of F implies that the choice of tile containing the dotted edge does not matter, so we continue to discuss T_4 without loss of generality, using Figures 2.9 and 2.10 for visual reference. Consider the graph G obtained from F by adding a picture to each tile. Certainly each tile must have tile crossing number 0. Furthermore, T_4 must have two crossings when drawn as in Figure 2.9. For each of the two possibilities for a pair of crossing edges in the frame of T_4 in this drawing, the frame deforms continuously to one of the drawings of $T_4^{\updownarrow}$ or ${}^{\updownarrow}T_4$ given in Figure 2.10. With a picture added inside, consider an edge e both of whose endpoints are in T_4. We show the crossing number of a drawing in which some of the interior of e leaves the disk containing T_4 cannot be less than the crossing number of a drawing in which e lies entirely inside this disk. This implies each T_i must be 2-degenerate. Finally, we demonstrate that filling each tile of F with one of the pictures in Figure 1.3 gives a graph with crossing number 2.

In the following discussion, we define contraction of a disk in a drawing on the projective plane. We remark that, in general, edge-contraction in a drawing of a graph is not well-defined although this contraction operation, in this very particular context, is well-defined. Let $\Gamma(F)$ be a 1-drawing of F in which T_4 is twisted, so the single crossing is between two edges of the frame of T_4. Let D be a disk surrounding T_4 (and including no other vertices) in such a drawing, as shown in Figure 2.11. Generate a new drawing $\Gamma'(H)$ of $H = F/E(T_4)$ as follows. Delete all vertices of T_4 and place a new vertex x in the interior of D. Add edges between x and each vertex of T_3 and T_5 that has a neighbor in T_4, such that the cyclic sequence of neighbors of x matches the order of these vertices in a walk around the boundary of D. The resulting drawing $\Gamma'(H)$ is a representativity-2 embedding of $F/E(T_4)$, as it contains a representativity-2 drawing of K_4. Thus we see $G/E(T_4)$ has representativity 2 on the projective plane. This implies that if an edge between two vertices of T_4 is added to F and crosses the boundary, this edge crosses at least one other edge of F. Similarly, we consider replacement of D by a 6-cycle whose vertices are ordered around the cycle to correspond to the orientation within D of the points of attachment of T_4 to the rest of F. If an edge e whose endvertices lie in D is drawn in this graph with the interior of e not locally homotopic to a drawing in D, this edge must cross another edge of F. If an edge of a picture inside T_4 contributes one to the crossing number of G when drawn inside D, drawing e outside D does not decrease the crossing number of the drawing. We may thus restrict ourselves to considering tile drawings of the tiles of G. Furthermore, we conclude from Lemma 1.2 that a tile of F may be a sequence of 2-degenerate tiles. In particular, since $T_i \otimes^{\updownarrow} T_{i+1}^{\updownarrow} \otimes T_{i+2}$ is a tile, we may consider a graph with only six tiles without loss of generality, though $\mathcal{T}$ may have any length at least six.

We are now prepared to prove the main result of this chapter.

Theorem 2.4. *The graphs in $\mathcal{T}_a^+(\mathcal{S})$ form an infinite family of 3-connected, 2-crossing-critical graphs for the projective plane.*

Proof. Let G be a graph in $\mathcal{T}_a^+(\mathcal{S})$. Lemma 2.2 shows the crossing number of G on the projective plane is at least two. In the proof of Lemma 2.2 we see that in an optimal drawing of G on the projective plane all tiles but one are embedded in a tile drawing with no crossings. The remaining tile T is drawn in a tile drawing of $T^{\updownarrow}$ or ${}^{\updownarrow}T$, so the 2-crossing-criticality of G follows from the 2-degeneracy of T. □

2.3 The Asymmetric Cases

The previous discussion focused on members of the family $\mathcal{T}_a^+(\mathcal{S})$, in which the vertex added to the circular ladder attaches to alternating even- and odd-indexed tiles. We now turn to two remaining cases that allow removal of the restriction that indices of tiles containing neighbors of the vertex off the tile belt alternate.

Definition 2.5. *Let $\mathcal{T}$ be a sequence $\left(T_0, {}^{\updownarrow}T_1^{\updownarrow}, T_2 \ldots, T_{2m}, {}^{\updownarrow}T_{2m+1}^{\updownarrow}\right)$ of tiles in $\mathcal{S}$ for $m \geq 2$. For each i from 0 to $2m+1$ let v_i be the frame vertex incident to the right dotted edge in Figure 1.2 that is identified with a vertex of the picture inside T_i. Define $\mathcal{T}^+(\mathcal{S})$ to be the set of graphs obtained by adding to $\circ(\otimes\mathcal{T})$ a vertex v adjacent to v_i for each of three even values and each of three even values of i.*

We note that $\mathcal{T}_a^+(\mathcal{S}) \subset \mathcal{T}^+(\mathcal{S})$, so we need only consider the two cases in which the neighbors of v do not have indices of alternating parity. Each of the frameworks in the remaining cases has a minor isomorphic to F1, and we will demonstrate the graphs have crossing number 2. The branch vertices of a spanning $\mathcal{U}$ subgraph in each case are marked with triangles.

In the second case, the framework F has two crossings in five of the six embeddings of its spanning $\mathcal{U}$ subgraph. Since F has an $F1$ minor, we know every drawing of F in the projective plane has at least one crossing.

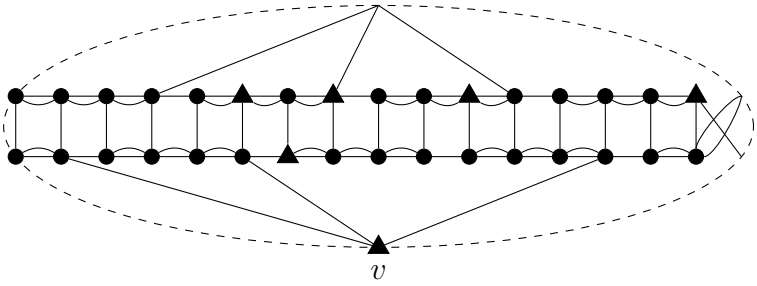

Figure 2.12. The second set of points of attachment.

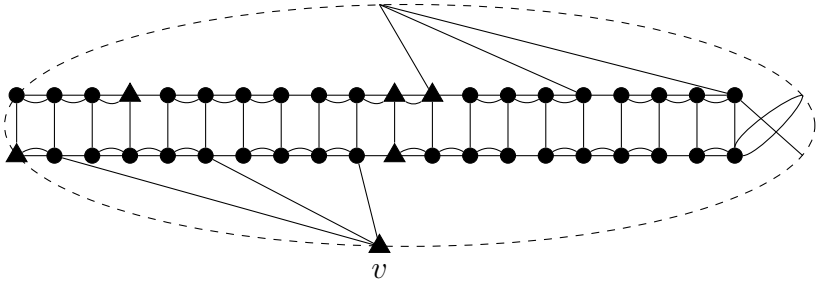

Figure 2.13. The third set of points of attachment.

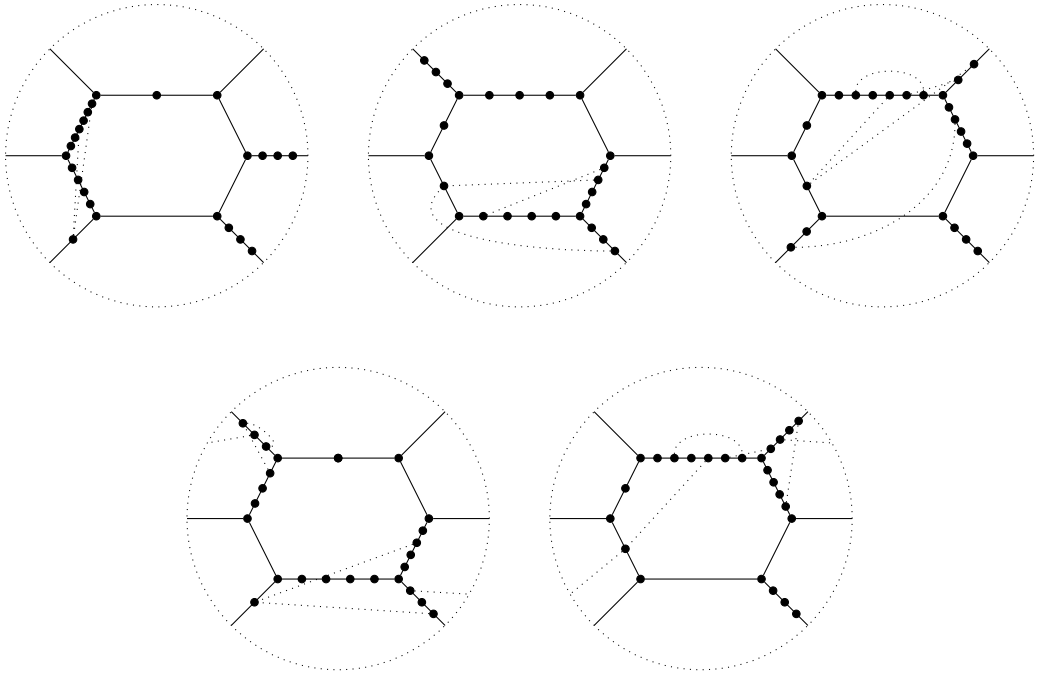

Figure 2.14. Five of the six embeddings of $\mathcal{U}$ in the second case lead to at least two crossings in an empty framework.

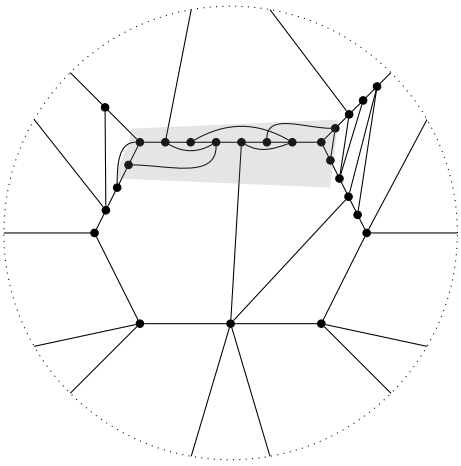

Figure 2.15. A 1-drawing of F with a disk containing the crossing highlighted.

The sixth embedding in this case has multiple 1-drawings, but all are localized to three consecutive tiles. In particular, we see the vertices that bound these tiles in sequence along the 6-cycle of the $\mathcal{U}$ subgraph of the framework are restricted to a right-inverted tile drawing. As we have established the right-inverted tile drawing of each tile filled with one of the pictures in Figure 1.3 has tile crossing number 2, we will see the graph G obtained by filling each of the tiles with one of these pictures has projective crossing number 2.

If we contract a disk D surrounding these tiles to a single point, the resulting drawing has representativity 2. No edge of a crossing in D can be redrawn passing through the boundary without contributing at least one crossing to the drawing, so we need only consider drawings in which edges incident to two vertices in D are represented by nulhomotopic simple closed curves when we contract D to a single point. We know a tile drawing of these three tiles has tile crossing number 2, so we consider only drawings that are not locally homeomorphic to tile drawings in D. If such a drawing has a single crossing, then this crossing must involve an edge of the three tiles of interest and an edge outside D, so it is possible to draw G with the given embedding of the $\mathcal{U}$ subgraph with no crossings in D. Since the framework has a non-projective minor, every drawing of F has at least one crossing; we have

shown that crossing must occur within D. It follows that the subgraph of G whose frames are drawn in the highlighted region in Figure 2.15 must be drawn with a crossing locally homeomorphic to a crossing in D, so a crossing elsewhere will be a second crossing. In this case, as in the case of a tile drawing, we see G has crossing number 2.

Chapter 3
2-Crossing-Critical Graphs on Non-orientable Surfaces

In this chapter we use the family $\mathcal{T}^+(\mathcal{S})$ of 2-crossing-critical graphs on the projective plane and the family $\mathcal{T}(\mathcal{S})$ of graphs that are 2-crossing-critical on the plane to construct for each non-orientable surface a family of graphs that are 2-crossing-critical on that surface.

Recall from Chapter 1 the set of twisted tile belts $\mathcal{T}(\mathcal{S})$. This set contains all 3-connected 2-crossing-critical graphs on the plane with a subdivision of V_{10}. For $i \geq 1$, let $\mathcal{T}_i(\mathcal{S})$ be the union of a graph from $\mathcal{T}^+(\mathcal{S})$ with $i-1$ graphs from $\mathcal{T}(\mathcal{S})$. We will show that all members of $\mathcal{T}_i$ are 2-crossing-critical on the non-orientable surface of genus i for each $i \geq 2$. Since $\mathcal{T}^+(\mathcal{S}) = \mathcal{T}_1(\mathcal{S})$, we have already demonstrated this result for $i = 1$.

3.1 Non-Orientable Surfaces

In the following discussion we concern ourselves with curves in non-orientable surfaces and with the relationships between those curves and the drawings of graphs. We provide some necessary definitions and observations about these curves and surfaces.

If X is a topological space, a *closed curve* in X is a mapping $f : [0,1] \to X$ with $f(0) = f(1)$. If the restriction of f to $[0,1)$ is one-to-one, we say f is *simple*.

If the complement of a simple closed curve f on a surface is disconnected, we call f a *separating curve* and refer to the components of the complement of f as the *inside* and *outside* of the curve. If at least one of the inside or outside of f is homeomorphic to a disk, then f is a *contractible* curve, otherwise f is *non-contractible*.

Given a point x on a simple closed curve f on a surface Σ, assign a local orientation to a neighborhood of x in Σ. If the orientation at x remains unchanged

after traversing f, then f is an *orientation-preserving curve*. If the orientation at x is reversed after traversing f, then f is an *orientation-reversing curve*.

We use *fundamental polygons* to construct non-orientable surfaces. The non-orientable surface of genus g, denoted $\mathbb{N}_g$, is obtained from a $(2g)$-gon whose sides are numbered consecutively from 0 to $2g-1$ by assigning the same orientation to each side and identifying sides $2k$ and $2k+1$ for k from 0 to $g-1$. Each pair of identified sides forms a closed curve; denote these curves $\alpha_0, \alpha_1, \ldots, \alpha_{g-1}$. We observe $\alpha_k(1) = \alpha_0(1)$ for all k. Let $x_0 = \alpha_0(1)$; we recall the fundamental group $\pi(\mathbb{N}_g)$ is the free group on generators $\alpha_0, \alpha_1, \ldots, \alpha_{g-1}$ subject to the relation $\alpha_0\alpha_1 \cdots \alpha_{g-1} = 1$. If f is a closed curve in $\mathbb{N}_g$ freely homotopic to some $\sigma \in \pi(\mathbb{N}_g)$ we call f a σ-curve.

We shall first consider drawings on the Klein bottle of graphs from $\mathcal{T}_2(\mathcal{S})$, then apply some topological results to reduce the question of crossing number on higher-genus non-orientable surfaces to crossings on $\mathbb{N}_2$.

3.2 2-Crossing-Critical Graphs

We observe first that given a drawing of a graph on a Möbius band we obtain a drawing with the same edge crossings on the projective plane by gluing a disk to the boundary of the Möbius band and contracting the disk to a point. Similarly, given a drawing of a graph on the projective plane we obtain a drawing on a Möbius band by deleting an open disk in the complement of the drawing's image. Thus in addition to illustrating a 2-drawing on the projective plane of a graph in $\mathcal{T}^+(\mathcal{S})$, the drawing in Figure 2.2 illustrates a 2-drawing of this graph on a Möbius band. It is easy to see that graphs in $\mathcal{T}(\mathcal{S})$ can be embedded in a Möbius band.

In [28], the authors provide some insight into the drawing of 1-vertex-connected and disconnected graphs through examination of their blocks. A graph G is *orientably simple* if its orientable genus $\gamma(G)$ is less than half its non-orientable genus

$\tilde{\gamma}(G)$, that is, if $\gamma(G) < \frac{1}{2}\tilde{\gamma}(G)$. We remark that Theorem 3.1 and Lemma 3.2 are still valid if we replace 'blocks' with 'components' and remove the requirement that the graph be connected.

Theorem 3.1. *A connected graph is orientably simple if and only if all of its blocks are orientably simple.*

Consider a graph $G = G_1 \cup G_2$ embedded in a non-orientable surface Σ of genus $\tilde{\gamma}(G)$. Let σ be a simple closed curve in Σ that separates G_1 and G_2; remove from Σ an open neighborhood of σ. Then the boundary of each of the components of the disconnected surface obtained in this way is contained in a face of the component of G embedded therein. We mark a vertex of each G_i from the face containing the boundary and create the graph G' by identifying the marked vertex of G_1 with the marked vertex of G_2. We obtain from the embedding of G an embedding of connected G' in Σ with $k(G') = k(G) - 1$. We repeat this process until we obtain a connected graph H whose blocks are precisely the blocks of G.

Since all components of $\mathcal{T}_i(\mathcal{S})$ are orientably simple for $i \geq 1$, we may apply the following lemma.

Lemma 3.2. *Let $G_1, \cdots, G_n$ be blocks of the connected graph G. If G is orientably simple, then*

$$\tilde{\gamma}(G) = 1 - n + \sum_{i=1}^{n} \tilde{\gamma}(G_i),$$

otherwise,

$$\tilde{\gamma}(G) = 2n - \sum_{i=1}^{n} \max\{2 - 2\gamma(G_i), 2 - \tilde{\gamma}(G_i)\}.$$

In [16], the authors are focused on finding 2-crossing critical graphs with a vertex of high degree, in particular on the projective plane. They generalize their result to higher-genus non-orientable surfaces; our result generalizes analogously with the following theorem.

Theorem 3.3. *Let $\mathcal{T}_g(\mathcal{S})$ be the set of graphs $H_1 \cup H_2 \cup \cdots \cup H_g$ with $H_1 \in \mathcal{T}^+(\mathcal{S})$ and $H_k \in \mathcal{T}(\mathcal{S})$ for $k \geq 2$. If $G \in \mathcal{T}_g(\mathcal{S})$, then G is 2-crossing critical on $\mathbb{N}_g$.*

We make use of the following two results from [15].

Lemma 3.4. *Let N be a compact connected nonorientable surface. Then there is a unique integer $p > 0$ such that N contains p, but not $p+1$, disjoint Möbius bands.*

The integer p in the theorem above is called the *Möbius number* of the surface N.

Lemma 3.5. *Let N be a compact connected nonorientable surface without boundary, having Möbius number p. Then N is a nonorientable surface of genus p.*

We apply these two results to a graph $G \in \mathcal{T}_g(\mathcal{S})$, first establishing the crossing number on $\mathbb{N}_g$ of G in Lemma 3.6 then demonstrating criticality of that crossing number in Lemma 3.7.

Lemma 3.6. *If $G \in \mathcal{T}_g(\mathcal{S})$, then $\mathrm{cr}_{\mathbb{N}_g}(G) = 2$.*

Proof. Let G be a graph in $\mathcal{T}_g(\mathcal{S})$ consisting of components $H_1 \in \mathcal{T}^+(\mathcal{S})$ and H_2 to H_g in $\mathcal{T}(\mathcal{S})$. Draw H_1 on a Möbius band with two crossings and embed each of H_2 to H_g in distinct Möbius bands. We may only embed the Möbius bands with no two crossing in a non-orientable surface of genus at least g, implying G has crossing number at most 2 on $\mathbb{N}_g$.

We know G cannot be embedded in $\mathbb{N}_g$, for the sum of the non-orientable genera of its components is $g+1$. Now suppose $\Gamma(G)$ is a 1-drawing on $\mathbb{N}_g$. We examine two cases, depending on whether both of the crossing edges are edges of H_1. If so, then all other components of G are embedded so each contains a noncontractible cycle. Let w be an element of the fundamental group of surface Σ. If D is a drawing of a graph on Σ and C a cycle in the graph such that D embeds C along a w-curve,

we refer to $D(C)$ (or to C, if context is clear) as a w-cycle. We may, without loss of generality, suppose these are $\alpha_1, \alpha_2, \ldots, \alpha_{g-1}$-cycles where

$$\pi(\mathbb{N}_g, x_0) = \left\langle \alpha_0, \alpha_1, \ldots, \alpha_{g-1} \mid \prod_0^{g-1} (\alpha_i^2) = 1 \right\rangle.$$

If the cycles correspond to longer words from the fundamental group, some will cross. Cutting along these cycles leaves only α_0-cycles (or cycles drawn freely homotopically to α_0-cycles) as candidates for noncontractible cycles in $\Gamma(H_1)$. This would, however, imply H_1 has a 1-drawing in $\mathbb{N}_1$, contradicting Theorem 1.10.

If at least one edge of the single crossing pair is in $G \backslash H_1$, then $\Gamma(H_1)$ is an embedding of H_1 in $\mathbb{N}_g$. Since H_1 is not projective, $\Gamma(H_1)$ contains (without loss of generality) an $\alpha_0\alpha_1$-curve or a disjoint pair of an α_0-curve and an α_1-curve. In fact, since H_1 is 3-connected, Menger's Theorem implies this embedding has an $\alpha_0\alpha_1$-curve. As before, we see $g-2$ of the remaining components are embedded, with $\alpha_2, \alpha_3, \ldots, \alpha_{g-1}$-cycles in these components. Without loss of generality, suppose H_g contains an edge from the crossing. Since H_g cannot be 1-drawn on a disk, the drawing of H_g must include an orientation-reversing curve. This cannot be an α_k-curve for $k \geq 2$, for such a curve would intersect at least twice a representativity-2 embedded graph in a Möbius band.

Certainly H_g cannot have an α_0-cycle and an α_1-cycle, for each would cross the $\alpha_0\alpha_1$-cycle of H_1, giving at least two crossings. Similarly, an $\alpha_0\alpha_1\alpha_0$ (or longer) cycle would cross the $\alpha_0\alpha_1$-cycle of H_1 at least twice. We conclude that all orientation-reversing curves in the drawing of H_g are without loss of generality α_0-cycles. This implies H_g is drawn on a Möbius band with at most one crossing. But H_g has representativity 2 on the projective plane, so an embedding would cross the $\alpha_0\alpha_1$-cycle of H_1 at least twice. If H_g is drawn with one crossing on a Möbius band,

then $\Gamma(H_g)$ still has an orientation-reversing curve, for the plane crossing number of H_g is two. This curve intersects the $\alpha_0\alpha_1$-curve of H_1 for a second crossing. □

The final step in proving Theorem 3.3 is to establish criticality of the crossing number.

Lemma 3.7. *If $G \in \mathcal{T}_g(\mathcal{S})$, then $\mathrm{cr}_{\mathbb{N}_g}(G\backslash e) < 2$ for each edge e of G.*

Proof. Let H_1 to H_g be the components of G as in the proof of Lemma 3.6. If e is an edge of H_1, then since H_1 is 2-crossing-critical on the projective plane, there is a 1-drawing or an embedding of $H_1\backslash e$ in a Möbius band. Each of the remaining components can be embedded in a Möbius band; Lemmas 3.4 and 3.5 show these g Möbius bands are embeddable in $\mathbb{N}_g$ with no two crossing. We have now a drawing of $G\backslash e$ with at most one crossing. If e is an edge of some other H_k (without loss of generality say H_2), then we invoke the plane 2-crossing-criticality of H_2 to draw $H_2\backslash e$ on a disk with at most one crossing. Embed H_3 to H_g in $g-2$ Möbius bands and embed H_1 in a Klein bottle; these $g-1$ surfaces may be disjointly embedded in $\mathbb{N}_g$. Embedding the disk containing $H_2\backslash e$ in the complement of the other components' drawings completes a drawing in $\mathbb{N}_g$ of $G\backslash e$ with at most one crossing. □

Chapter 4
2-Crossing-Critical Graphs on Orientable Surfaces

In this chapter we construct for each orientable surface of positive genus an infinite family of 2-crossing-critical graphs. These graphs are constructed from 3-connected 2-crossing-critical graphs on the plane and have a number of 2-separations equal to the genus of the surface on which they are 2-crossing-critical. We first consider the torus, then use an inductive construction to give 2-crossing-critical graphs for each surface of higher genus.

4.1 The Torus

In this section we examine the torus crossing number of a 2-amalgamation of two graphs from $\mathcal{T}(\mathcal{S})$. The main result of this section is the following theorem:

Theorem 4.1. *Let G_1 and G_2 be graphs in $\mathcal{T}(\mathcal{S})$ and let the endvertices of a single exterior frame edge in each G_i be labeled x and y. Then the graph G obtained by identifying the edges xy in G_1 and G_2 is 2-crossing-critical on the torus.*

We first show G has genus 2, implying $cr_{\mathbb{S}_1}(G) \geq 1$, then show no embedding of (without loss of generality) G_1 in the torus can be extended to a 1-drawing of G.

4.1.1 2-Amalgamations

We employ notation and the following definition from [6]:

Definition 4.2. *Given two graphs G_1 and G_2 with $V(G_1) \cap V(G_2) = \{x, y\}$ and $E(G_1) \cap E(G_2) = \varnothing$, the* 2-amalgamation $G_1 \bigcup_{\{x,y\}} G_2$ *of G_1 and G_2 has vertex set $V(G_1) \cup V(G_2)$ and edge set $E(G_1) \cup E(G_2)$.*

We remark that if x and y are adjacent in both G_1 and G_2, the 2-amalgamation will introduce parallel edges between x and y.

For a graph G with vertices x and y, define G' to be $G \bigcup_{\{x,y\}} K_2$ and G'' to be $G \bigcup_{\{x,y\}} K$ where K is obtained by subdividing two non-consecutive edges of K_5 and

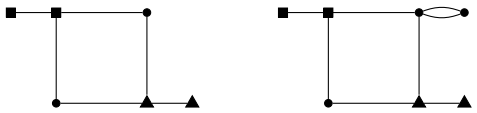

Figure 4.1. Choices for vertices to label x and y.

labeling the degree-two vertices x and y. If x and y are adjacent in G, then G' will be a multigraph of (orientable) genus $\gamma(G)$ but construction of G'' will not introduce any parallel edges not present in G.

The relations among the genera of G, G', and G'' determine how the structure of G impacts the genus of its 2-amalgamation with another graph H, as described by the function $\mu(G) = 3 + 2\gamma(G) - \gamma(G') - \gamma(G'')$. Given two graphs G and H, we define the function $\varepsilon(G, H) = \left\lceil \frac{3-\mu(G)\mu(H)}{4} \right\rceil$. With these functions in hand, we can state the following theorem from [6]:

Theorem 4.3. $\gamma(G_1 \underset{\{x,y\}}{\cup} G_2) = \gamma(G_1) + \gamma(G_2) + \varepsilon(G_1, G_2)$.

For the torus, we will consider two graphs G_1 and G_2 from $\mathcal{T}(\mathcal{S})$ with either the square pair or the triangular pair of vertices shown in Figure 4.1 labeled x and y in each. In the following section we will show the graph $G_1 \underset{\{x,y\}}{\cup} (G_2 - xy)$ is 2-crossing-critical on the torus.

4.1.2 2-Crossing-Criticality

For simplicity, let $G = H_1 \underset{\{x,y\}}{\cup} H_2$ be the 2-amalgamation of two graphs as described in the previous section with $H_1 = G_1$ and $H_2 = G_2 - xy$. We begin the section by showing $\gamma(G) = 2$, then proceed to produce a contradiction when attempting to construct a 1-drawing of G on the torus.

We first make observations about the genera of graphs used to define $\mu(H_1)$ and $\mu(H_2)$. Since H_1 and H_2' are in $\mathcal{T}(\mathcal{S})$ and x and y are adjacent in H_1, we know $\gamma(H_1)$, $\gamma(H_1')$, and $\gamma(H_2')$ are all 1. That $\gamma(H_2) = 0$ is established in [2]. Let H be the graph obtained from V_8 by removing an edge on the rim cycle of the Möbius ladder and labeling its endvertices x and y; the graph H'' has genus 2 and

is a minor of both H_1'' and H_2'', so $\gamma(H_1'') \geq 2$ and $\gamma(H_2'') \geq 2$, and in fact both graphs have genus 2.

These results allow us to compute $\mu(H_1) = 2$ and $\mu(H_2) = 0$, so $\varepsilon(H_1, H_2) = 1$. By Theorem 4.3 we see $\gamma(G) = 2$, implying $cr_{\mathbb{S}_1}(G) \geq 1$. Now we observe that both G_1 and G_2 are subgraphs of G since one copy of xy is retained in G.

Suppose there exists a 1-drawing Γ of G on the torus; then at least one G_i (without loss of generality, say G_1) is embedded. Since $\gamma(G_1) = 1$, the restriction of Γ to G_1 is a cellular embedding. If this embedding is extended to a drawing $\Gamma(G)$ with all of $H_2 - H_1$ drawn in a single face of $\Gamma(H_1)$, then the restriction to $\Gamma(G_2)$ gives a drawing of G_2 in a disk. Such a drawing must have two crossings, so we see that in each torus 1-drawing $\Gamma(G)$, both restrictions $\Gamma(G_1)$ and $\Gamma(G_2)$ are embeddings.

It follows that in a 1-drawing $\Gamma(G)$, the unique crossing must be an edge e of $H_1 - \{xy\}$ crossing an edge f of H_2. Suppose $f = uv$; then u and v lie in distinct faces of $\Gamma(G_1)$. Since H_2 is 2-connected, there is a uv-path in H_2 that avoids f; such a path must cross a boundary edge in each of the faces of $\Gamma(H_1)$ containing u and v, contradicting the uniqueness of the e, f-crossing. We see, then, that there can be no 1-drawing of G on the torus, so $cr_{\mathbb{S}_1}(G) \geq 2$. Since both G_i have plane crossing number 2, we see an embedding η of H_1 in the torus can be extended to a 2-drawing $\eta(G)$ in which H_2 is drawn in a face of $\eta(H_1)$ whose boundary includes the edge xy.

Criticality follows easily from the 2-drawing of G_2 in a disk; removal of an edge of H_2 (or, by symmetry, an edge of H_1) leaves a graph with at most one crossing as implied by Theorem 1.10.

4.2 Orientable Surfaces of Higher Genus

In this section we show that the method used in the previous section to construct 2-crossing critical graphs on the torus with a unique 2-separation may be extended to an orientable surface of genus g. Such a graph, built from the 2-crossing-critical tile belts on the plane, has g 2-separations. We remark that construction of connectivity-1 and disconnected 2-crossing-critical graphs is not immediate, as the question of whether one can always draw a disconnected graph optimally with no edge crossings between two components is still open for orientable surfaces of genus at least 2.

4.2.1 Inductive Construction

In this section we construct for each $g \geq 1$ a set of graphs that are 2-crossing-critical on $\mathbb{S}_g$.

Definition 4.4. *For $k \geq 1$ let $G_1, G_2, \ldots G_{k+1}$ be graphs in $\mathcal{T}(\mathcal{S})$. In G_i label the endpoints of a dotted frame edge x_i and y_i for i from 1 to $k+1$; for j from 2 to $k+1$ label the endpoints of a dotted frame edge x_{j-1} and y_{j-1} so in G_i the sets $\{x_{j-1}, y_{j-1}\}$ and $\{x_j, y_j\}$ are disjoint. For each $i \geq 2$ define G_i^- to be the graph obtained from G_i by deleting the edge $x_{i-1}y_{i-1}$. Let $\mathcal{B}_1(\mathcal{S})$ be all graphs $G_1 \bigcup_{\{x_1,y_1\}} G_2^-$ and for $k \geq 2$ let $\mathcal{B}_k(\mathcal{S})$ be all graphs $H_{k-1} \bigcup_{\{x_k,y_k\}} G_{k+1}^-$ where $H_{k-1} \in \mathcal{B}_{k-1}(\mathcal{S})$.*

We proved in the previous section that graphs in $\mathcal{B}_1(\mathcal{S})$ are 2-crossing-critical on the torus. Observe that a graph in $\mathcal{B}_k(\mathcal{S})$ has a subgraph isomorphic to G_i for each i from 1 to k since one copy of each edge x_i, y_i is preserved in the sequential 2-amalgamations. The primary result of this section is the following theorem.

Theorem 4.5. *If $G \in \mathcal{B}_g(\mathcal{S})$, then G is 2-crossing-critical on $\mathbb{S}_g$.*

The proof is split into two parts: we establish the crossing number in the next section then establish criticality in the following section.

4.2.2 Crossing Number 2

We prove each graph G in $\mathcal{B}_g(\mathcal{S})$ has crossing number 2 on the orientable surface $\mathbb{S}_g$ by first proving inductively that $\gamma(G) = g+1$. We then show that, if G is the 2-amalgamation of a graph H_1 in $\mathcal{B}_g(\mathcal{S})$ and H_2 in $\mathcal{T}(\mathcal{S})$, the lack of an $x_g y_g$-alternating genus embedding of H_1 prohibits any 1-drawing of G on $\mathbb{S}_k$. We prove Theorem 4.5 in two steps, starting with the following lemma.

Lemma 4.6. *If $G \in \mathcal{B}_g(\mathcal{S})$, then $cr_{\mathbb{S}_g}(G) = 2$.*

Proof. The case $g = 1$ is proved in Theorem 4.1. Now let g be at least 2 and suppose $G \in \mathcal{B}_g(\mathcal{S})$ is the 2-amalgamation of $H_1 \in \mathcal{B}_{g-1}(\mathcal{S})$ and $H_2 = G_2^-$ for $H_2 \in \mathcal{T}(\mathcal{S})$ on the vertices x_g and y_g. Suppose $\gamma(H_1) = g$ and $cr_{\mathbb{S}_{g-1}}(H_1) = 2$. If H_1 has an $x_g y_g$-alternating embedding in $\mathbb{S}_g$, then graphs in $\mathcal{T}(\mathcal{S})$ have an xy-alternating embedding in the torus for the endvertices x and y of each dotted frame edge. Since this is not the case, with $x_g y_g$ the terminals of H_1 we have $\mu(H_1) = 2$. This implies $\gamma(G) \geq g+1$. Since $\gamma(H_1) = g$ and $\gamma(H_2) = 1$ we conclude $\gamma(G) = g+1$.

If neither H_1 nor H_2 is embedded in a drawing of G in $\mathbb{S}_g$, then such a drawing has at least two crossings. Let $\Gamma(G)$ be a drawing in $\mathbb{S}_g$ and suppose the restriction of Γ to H_1 is an embedding. If $\Gamma(G)$ is a 1-drawing, then either the restriction of Γ to H_2 is a 1-drawing in a face of $\Gamma(H_1)$ or Γ embeds H_2 and one edge of H_2 crosses one edge of H_1. In the first case, $\Gamma(H_2)$ would be a 1-drawing of H_2 in a disk since H_1 has no $x_g y_g$-alternating embedding in $\mathbb{S}_g$, contradicting Theorem 1.10. In the second case, the endvertices of the crossing edge of H_2 are in two different faces of $\Gamma(H_1)$, so the 3-connectedness of H_2 implies a path P in H_2 between x_g and y_g that avoids the edge $x_g y_g$; the restriction of Γ to $H_1 \cup P$ must have at least one crossing, contradicting the supposition that $\Gamma(G)$ is a 1-drawing.

Now let $\Gamma(G)$ be a drawing in $\mathbb{S}_g$ and suppose the restriction of Γ to H_2 is an embedding. We have seen already that Γ may not also embed H_1 without at least two crossings between edges of H_1 and edges of H_2, so suppose $H_1 - x_g y_g$ is 1-drawn in $\mathbb{S}_g - \Gamma(H_2)$. Since by inductive assumption H_1 has crossing number 2 on $\mathbb{S}_{g-1}$, it must be the case that $\Gamma(H_2)$ is an $x_g y_g$-alternating embedding. Since $\mu(H_2) = 2$, we know $\Gamma(H_2)$ is an embedding in a surface of genus at least 2, implying the extension of the 1-drawing of $H_1 - x_g y_g$ to H_1 is a 1-drawing on a surface of genus $g-1$. This contradicts the inductive hypothesis, so Γ must have at least two crossings, that is, $\mathrm{cr}_{\mathbb{S}_g}(G) \geq 2$.

To show $cr_{\mathbb{S}_g}(G) = 2$, we begin with a genus embedding $\Gamma(H_1)$. This is a 2-cell embedding that is, as we have seen, not $x_g y_g$-alternating. It follows from the proof of Theorem 1.10 that there is a 2-drawing of H_2 in a disk that has $x_g y_g$ crossing no other edge. Let P be a path between x_g and y_g in this disk disjoint from the drawing of H_2 and P' a path between x_g and y_g in $\mathbb{S}_g$ disjoint from $\Gamma(H_1)$. Cut out the disks bounded by $x_g y_g P$ and $x_g y_g P'$ and identify their boundaries to obtain a 2-drawing of G on $\mathbb{S}_g$. □

4.2.3 Criticality

In this section we give a construction for critically 2-drawing in $\mathbb{S}_g$ an element of $\mathcal{B}_g(\mathcal{S})$. In particular, we prove the following lemma, which completes the proof of Theorem 4.5.

Lemma 4.7. *If $H_g \in \mathcal{B}_g(\mathcal{S})$, then $\mathrm{cr}_{\mathbb{S}_g}(H_g \backslash e) < 2$ for each edge e of G.*

Proof. Suppose $\Gamma'(G)$ is a 1-drawing in the plane of a graph G with a single pair uv and yz of crossing edges. Then the restriction of Γ' to $G \backslash \{uv, yz\}$ is an embedding in which one face F contains u, v, y, and z ordered either $uyvz$ or $uzvy$ in the facial walk. A *planarization* of Γ' is an embedding $\Gamma(G)$ obtained by deleting uv and yz

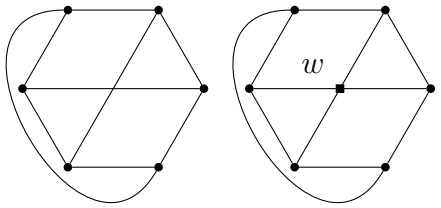

Figure 4.2. A planarization of $K_{3,3}$. Note the endvertices of the crossing edges alternate in the ordering of neighbors about w.

and adding a new vertex w in F with neighbors u, v, y , and z. This construction is an *uncrossing* of uv and yz. The rotation of w's neighbors in Γ is either $uyvz$ or $uzvy$. To *reverse* this uncrossing, delete w and add edges uv and yz with both their interiors in the face of $\Gamma'(G \setminus \{uv, yz\})$ in which w was added. We may obtain in this way a planarization of a k-drawing of a graph G by at most k uncrossings.

First we describe a planarization of a 2-drawing of a graph G_1 in $\mathcal{T}(\mathcal{S})$ and show that for each edge e of G_1 there is a planarization $P_0(G; e)$ in which each uncrossing includes e or one of its remnants. We next define an embedding in the torus of the 2-amalgamation H_1 of $P_0(G_1; e)$ with another graph G_2 in $\mathcal{T}(\mathcal{S})$ (minus the edge whose endvertices are the markers for the 2-amalgamation). In general, we denote by $P_g(G; e)$ a graph obtained from G by at most 2 uncrossings, at least one of which involves e, if the resulting graph embeds in $\mathbb{S}_g$. Note that such graphs are only well-defined if $G \setminus e$ has crossing number at most 1 on $\mathbb{S}_g$. Finally, we describe how to extend the graph corresponding to a planarization $P_0(G; e)$ of $G \in \mathcal{T}(\mathcal{S})$, starting from a 2-drawing, to $P_g(H; e)$ where $H \in \mathcal{B}_g(\mathcal{S})$ and G is an induced subgraph of H. An embedding of $P_g(H; e)$ will therefore correspond to a 2-drawing of H in $\mathbb{S}_g$.

To see that $P_0(G; e)$ is well-defined for each edge e of $G \in \mathcal{T}(\mathcal{S})$, we refer the reader to the proof of Lemma 2.13 of [2]. The 2-drawings given there describe how

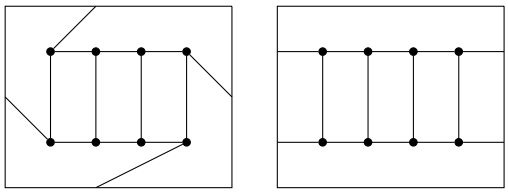

Figure 4.3. Torus embeddings of the Möbius ladder, left, and circular ladder, right, on 8 vertices.

to planarize a 2-drawing of a graph in $\mathcal{T}(\mathcal{S})$, once an edge is specified for uncrossing in the planarization. Notably such a graph will be an induced subgraph of some $G \in \mathcal{B}_g(\mathcal{S})$ containing all edges that cross in a 2-drawing of G. We note that the "top" and "bottom" vertices of tiles in such a planarization form two disjoint cycles so the tiles are embedded as in a circular ladder, rather than a Möbius ladder. We exploit this visual peculiarity to use as models for our 2-drawings a circular ladder and a Möbius ladder.

We first observe that since the twist in a Möbius band can be continuously perturbed along the band, when constructing an amalgamation H_1 of tile belts G_1 and G_2^- we may always choose the terminal vertices x and y so xy is not an edge of both the twisted tile of G_1 and the twisted tile of G_2^-. Let H_1 be an element of $\mathcal{B}_1(\mathcal{S})$ composed of tile belts G_1 and G_2 with terminal vertices x and y. Recall that both G_1 and G_2 are induced subgraphs of H_1. Let e be an edge of H_1; without generality we may assume e is an edge of G_1. Since G_1 is 2-crossing-critical on the plane, there is a planarization $P_0(G_1; e)$. Let $\Gamma_1(P_0(G_1; e))$ be an embedding in the plane and $\Gamma_2(G_2)$ an embedding in the torus. We remark that if $e = xy$, then $H_1 \backslash e$ is the 2-amalgamation of two planar graphs, which can always be embedded in the torus. Assume, therefore, that $e \neq xy$. We use the embeddings Γ_1 and Γ_2 to construct an embedding $\Gamma(P_1(H_1; e))$. For a vertex v of $P_0(G_1; e)$ other than x and y the order of v's neighbors in the rotation system for Γ is the same as in Γ_1. Similarly, for a vertex u of G_2 other than x and t the order of u's neighbors in

the rotation system for Γ is the same as in Γ_2. If the order of neighbors of x in the rotation system for Γ_1 is $y\sigma_1$ and the order of neighbors of x in the rotation system for Γ_2 is $\sigma_2 y$, the order of neighbors of x in the rotation system for Γ is $\sigma_1\sigma_2 y$. If the order of neighbors of y in the rotation system for Γ_1 is $x\rho_1$ and the order of neighbors of y in the rotation system for Γ_2 is $\rho_2 x$, the order of neighbors of y in the rotation system for Γ is $\rho_1\rho_2 x$. The graph $P_1(H_1; e)$ contains exactly two vertices not in $V(H_1)$, each of which corresponds to an uncrossing. Reversing these uncrossings in Γ gives a 2-drawing $\Gamma'(H_1)$ on the torus such that $\Gamma'(H_1\backslash e)$ has at most one crossing. Since we imposed no restriction on the choice of e, this demonstrates the criticality of the crossing number of H_1.

Let g be an integer at least 2; we follow this model given for $g = 1$ to construct for each edge of $H_g \in \mathcal{B}_g(\mathcal{S})$ a 2-drawing of H_g on $\mathbb{S}_g$ where e is a member of at least one crossing. Let H_{g-1} be an element of $\mathcal{B}_{g-1}(\mathcal{S})$ and G_{g+1} an element of $\mathcal{T}(\mathcal{S})$ so $H_g = H_{g-1} \bigcup_{\{x,y\}} G^-_{g+1}$. For an edge e of H_g, we consider three cases: $e = xy$, e is an edge of H_{g-1} other than xy, and e is an edge of G_{g+1} other than xy.

First, if $e = xy$, then $H_{g-1}\backslash e$ embeds in $\mathbb{S}_{g-1}$. The genus of $H_{g-1}\backslash e$ is $g-1$ and the genus of $G_{g+1}\backslash e$ is 0. Theorem 4.3 gives g as an upper bound for the genus of $H_g\backslash e$.

Next, suppose e is an edge of H_{g-1} other than xy. We assume for induction that there is an embedding Γ_1 in $\mathbb{S}_{g-1}$ of $P_{g-1}(H_{g-1}; e)$ with at most two uncrossings, at least one of which involves e. Let Γ_2 be an embedding in the torus of G_{g+1}. We construct from these embeddings an embedding Γ in $\mathbb{S}_g$ of $P_g(H_g; e)$ as follows. For a vertex v of $P_{g-1}(H_{g-1}; e)$ other than x and y the order of v's neighbors in the rotation system for Γ is the same as in Γ_1. Similarly, for a vertex u of G_{g+1} other than x and t the order of u's neighbors in the rotation system for Γ is the same as in Γ_2. If the order of neighbors of x in the rotation system for Γ_1 is $y\sigma_1$ and

the order of neighbors of x in the rotation system for Γ_2 is $\sigma_2 y$, then the order of neighbors of x in the rotation system for Γ is $\sigma_1\sigma_2 y$. If the order of neighbors of y in the rotation system for Γ_1 is $x\rho_1$ and the order of neighbors of y in the rotation system for Γ_2 is $\rho_2 x$, then the order of neighbors of y in the rotation system for Γ is $\rho_1\rho_2 x$. The graph $P_1(H_1; e)$ contains exactly two vertices not in $V(H_1)$, each of which corresponds to an uncrossing. Reversing these uncrossings in Γ gives a 2-drawing $\Gamma'(H_1)$ on the torus such that $\Gamma'(H_1\backslash e)$ has at most one crossing.

Finally, suppose e is an edge of G_{g+1} other than xy. Then there is an embedding Γ_2 of $P_0(G_{g+1}; e)$ in the plane with at most two uncrossings, at least one of which involves e. Let $\Gamma_1(H_{g-1})$ be an embedding in $\mathbb{S}_g$. The edge xy is on the boundary of a face of Γ_1 and a face of Γ_2; from each of these faces remove a disk whose intersection with the respective graph is the arc corresponding to xy. Identification of the boundaries of these disks such that the copies of xy are identified gives an embedding in $\mathbb{S}_g$ of $P_g(H_g; e)$ with at most two uncrossings, at least one of which involves e. Reversing these uncrossings gives a 2-drawing $\Gamma'(H_g)$ whose restriction to $H_g\backslash e$ has at most one crossing. With this final case, we see that $\mathrm{cr}_{\mathbb{S}_g}(H_g\backslash e) < 2$ for each edge e of a graph $H_g \in \mathcal{B}_g(\mathcal{S})$. □

Chapter 5
Hamiltonicity of Graphs on Surfaces

In this chapter we survey relevant results in hamiltonicity of graphs on surfaces. We note that in this discussion a number of results referenced prove results stronger than hamiltonicity; we recall here the hierarchy of hamiltonicity results. A graph is *path-hamiltonian* if it contains a hamilton path. A graph is *hamiltonian* if it contains a hamilton cycle; as removal of an edge from a hamilton cycle leaves a hamilton path, hamiltonicity implies path-hamiltonicity. A graph is *edge-hamiltonian* if for each edge of the graph there is a hamilton cycle that includes that edge. Clearly this implies the graph is hamiltonian. A graph is *hamilton-connected* if for each pair of vertices u and v in the graph there is a hamilton path with endvertices u and v. If u and v are adjacent we may extend this hamilton path to a hamilton cycle by addition of the edge uv, implying edge-hamiltonicity.

5.1 The Plane and the Projective Plane

In 1931, Whitney [38] showed that 4-connected triangulations of the plane are hamiltonian, beginning the rich study of hamilton cycles for graphs on surfaces. Thomassen [32] and Chiba and Nishizeki [5] extended this result by showing 4-connected planar graphs are hamilton-connected, and Thomas and Yu [29] showed 4-connected projective-planar graphs are hamiltonian. In the light of these results and what is known of the structure of 4-connected toroidal graphs, Grünbaum [14] and Nash-Williams [24] conjectured the following.

Conjecture 5.1. *Every 4-connected graph embeddable in the torus is hamiltonian.*

5.2 The Torus

A number of partial results for the torus are known. In [30], the hamiltonicity of 5-connected toroidal graphs is established. For 4-connected graphs, the nearest result, proved in [31], is that 4-connected toroidal graphs are path-hamiltonian.

Given the apparent difficulty of proving Conjecture 5.1, Ellingham and Marshall [8] have proposed a modification to the inductive approach used for the plane and projective plane in [29, 35, 36]. In particular, the results for the plane and projective plane are stronger than edge-hamiltonicity. A cycle C in a graph G is a *Tutte cycle* if every C-bridge of G has at most three attachments on C. The results for the plane and projective plane show that, given a facial cycle C of a plane (or projective plane) embedded graph G and an edge e of C, there is a Tutte cycle in G that includes e. In the 4-connected case, this implies edge-hamiltonicity. Ellingham and Marshall propose characterizing graphs on the torus that fail to be edge-hamiltonian. Thomassen gives 4-connected counterexamples to edge-hamiltonicity on the torus in [32]. These counterexamples consist of adding an edge with both endvertices in the same color class of a 4-connected bipartite embeddable graph. Ellingham and Marshall show that in the case of grid-type graphs on the torus, even a minor change from counterexamples like Thomassen's restores edge-hamiltonicity. In particular, they give the following result.

Theorem 5.2. *Let G be a 4-connected, 4-regular, bipartite simple graph on the torus with partition sets of white and black vertices. If we add a nonempty set E_1 of one or more black-black diagonals to G, then no element of E_1 lies on a hamilton cycle in $G \cup E_1$. However, if we add one further white-white diagonal e_2 in a quadrangle of $G \cup E_1$ then each edge of $G \cup E_1 \cup \{e_2\}$ lies on a hamilton cycle of that graph.*

Euler's formula implies that a 4-connected, 4-regular bipartite simple toroidal graph is a quadrangulation. All such quadrangulations of the torus can be defined by three integers m, n, and q. Let H be the Cartesian product of a path P_m and a cycle C_n. For $m \geq 2$ this graph contains two disjoint cycles of degree-three vertices.

Figure 5.1. A local domino transformation between quadrangulations.

Label the vertices of these cycles so one cycle is $v_0v_1 \dots v_{n-1}$ and the other cycle is $u_0u_1 \dots u_{n-1}$ and add edges v_ju_{j+q} for each $0 \leq j \leq n-1$ with addition modulo n to obtain a quadrangulation $Q(m, n; q)$ of the torus. For $m = 1$ the graph H is a cycle; label the vertices $v_0v_1 \dots v_{n-1}$ and add edges v_jv_{j+q} for each $0 \leq j \leq n-1$ with addition modulo n. All 4-regular 4-connected quadrangulations of the torus may be obtained (although not necessarily uniquely) by one of these constructions.

Ellingham and Marshall point out a transformation between quadrangulations that may reduce the connectivity, replacing the center edge of two consecutive quadrangles (a domino graph) with a long diagonal. We illustrate this *domino transformation* in Figure 5.1. In the case of a bipartite quadrangulation, a collection of transformations of this type may be followed by addition of a collection of edges all of whose endvertices are in the same color class to restore 4-connectedness. Such a graph will not be edge-hamiltonian, but addition of diagonals to quadrangles of a bipartite tiling creates a closely restricted family of counterexamples to edge-hamiltonicity. Suppose a graph has undergone a sequence of domino transformations and had edges added with all their endvertices in the same color class to restore 4-connectedness. It is not known whether addition of a single diagonal to a quadrangle of the resulting graph, with both its endvertices in the second color class, restores edge-hamiltonicity.

5.3 The Klein Bottle

We are concerned here with the following conjecture of Nash-Williams, given in [24].

Conjecture 5.3. *Every 4-connected graph embeddable in the Klein bottle is hamiltonian.*

Kawarabayashi reaffirms this conjecture in his 2001 survey [18], and this paper and Gould's 2014 survey reference a partial result for the Klein bottle analogous to Brunet and Richter's [4] first step for the torus, that 5-connected triangulations are hamiltonian [3]. Kawarabayashi [18] proposes that the triangulation condition may be replaced with a condition of sufficiently high representativity. While results on the torus have progressed to hamiltonicity of all 5-connected graphs [30] and existence of hamilton paths in every 4-connected graph [31], the Klein-bottle graphs for which these results are known are still only those that are also toroidal. In [32], Thomassen gives 4-connected counterexamples to edge-hamiltonicity of graphs embeddable in the Klein bottle. As with the torus, these counterexamples consist of adding an edge with both endvertices in the same color class of a 4-connected bipartite embeddable graph.

For the Klein bottle, there are three types of 4-connected bipartite 4-regular graphs. As on the torus, Euler's formula implies that these graphs are all quadrangulations. In the next chapter we will prove a result analogous to that of Ellingham and Marshall in two cases, explore their relationship via the domino transformation, and explore the edge-hamiltonicity of quadrangulations of the third type.

Chapter 6
Edge-hamiltonicity on the Klein Bottle

In this chapter we consider edge-hamiltonicity of 4-regular, 4-connected graphs embeddable in the Klein bottle. We focus on bipartite graphs, and observe that Euler's formula implies that 4-regular, 4-connected bipartite graphs that embed in the Klein bottle must be quadrangulations. We consider counterexamples to edge-hamiltonicity among 4-connected graphs and illustrate the criticality of these counterexamples, arguing that bipartiteness seems to be an essential property to consider when finding counterexamples to edge-hamiltonicity on the Klein bottle.

6.1 4-regular, 4-connected Klein Bottle Graphs

Quadrangulations of the Klein bottle are characterized in [33] and the 4-regular quadrangulations are characterized in [23] and grouped into three types: grid, ladder, and mesh. We address here bipartite members of the grid-type family $Q_g(p, r)$ and the ladder-type family $Q_l(2p, r)$. The first result of this chapter is the following theorem, which we prove in Section 6.2.

Theorem 6.1. *Let G be a bipartite grid-type quadrangulation of the Klein bottle with partition sets of white and black vertices. If we add a nonempty set E_1 of one or more black-black diagonals to the quadrangles of G, then no element of E_1 lies on a hamilton cycle in $G \cup E_1$. However, if we add one further white-white diagonal e_2 in a quadrangle of $G \cup E_1$, then each edge of $G \cup E_1 \cup \{e_2\}$ lies on a hamilton cycle of that graph.*

In Section 6.3 we prove the following result.

Theorem 6.2. *Let G be a bipartite ladder-type quadrangulation of the Klein bottle with partition sets of white and black vertices. If we add a nonempty set E_1 of one or more black-black diagonals to the quadrangles of G, then no element of E_1 lies*

on a hamilton cycle in $G \cup E_1$. However, if we add one further white-white diagonal e_2 in a quadrangle of $G \cup E_1$, then each edge of $G \cup E_1 \cup \{e_2\}$ lies on a hamilton cycle of that graph.

In Section 6.4 we describe the remaining family of 4-regular Klein bottle quadrangulations, identify its bipartite members, and show they are edge-hamiltonian. We observe that 4-connected counterexamples to edge-hamiltonicity arise from members of this family and discuss our approach to demonstrating criticality of such counterexamples.

6.2 Grid-type Quadrangulations

We follow the notation given in [23] to define the family $Q_g(p, r)$ of 4-regular quadrangulations of the Klein bottle, with a minor adjustment to indices for simplicity. To construct a graph in this family, place vertices at integer points in the plane from $(0, 0)$ to (r, p) and add all edges along line segments from $(i, 0)$ to (i, p) for $0 \leq i \leq r$ and line segments from $(0, j)$ to (r, j) for $0 \leq j \leq p$. Finally, identify $(i, 0)$ with (i, p) for $0 \leq i \leq r$ and add edges (with y-coordinates modulo p) between $(0, j)$ and $(r, p - 1 - j + n)$ for each j from 0 to $p-1$ and some non-negative integer $n < p$. After this identification, we will carry out all calculations involving y-coordinates modulo p. For visualization, we consider the fundamental polygon of the Klein bottle a rectangle bounding a neighborhood of $[0, r] \times [0, p - 1]$.

To construct bipartite graphs in this family, we require that p be even and that r and n have the same parity. We note that the examples used to show edge-hamiltonicity of bipartite graphs G in $Q_g(p, r)$ can also be used to show edge-hamiltonicity if p and r do not have the same parity. We shall refer to vertices by the coordinates (x, y) given in the initial construction and in the bipartite case color a vertex white if its coordinates are congruent modulo 2 and black otherwise.

We do not need to separately consider each equivalence class of edges under automorphisms of G, but make two observations about the symmetry of the graph. First, we observe that each edge $(i,0)$-$(i,p-1)$ is isomorphic to $(i,p/2)$-$(i,p/2-1)$. Second, observe (i,j)-$(i,j+1)$ is isomorphic to $(i,j-1)$-(i,j). These symmetries can easily be seen by drawing the graph in a fundamental polygon $abab^{-1}$ of the Klein bottle with $(0,0)$ near the bottom left corner and $(r,p-1)$ near the top right corner. To observe the first symmetry, shift the graph up $p/2$ units; to observe the second, shift the graph left 1 unit. We also note that increasing the y-coordinate of each vertex by 1 is a color-reversing automorphism of G that increases n by 2; combining this automorphism with the other two we may assume without loss of generality that n is equal to r mod 2. Since this fixes the value of n depending on the parity of r, we suppress n in the notation and discussion of graphs in this family.

Bearing in mind the symmetry described above, we present a hamilton cycle that uses (up to symmetry) every edge of G. First, traverse the horizontal segment of the grid on which G is drawn from $(0,0)$ to $(r,0)$, then move up to $(r,1)$ and back to $(0,1)$. Continue to move up exactly when "horizontal" edges would leave the grid, and this path will terminate at $(0,p-1)$ or $(r,p-1)$, depending on the parity of p (since we are focused on bipartite graphs, p is even) Since both $(0,p-1)$ and $(r,p-1)$ are adjacent to $(0,0)$, this describes a hamilton cycle. An example of such a hamilton cycle is shown in Figure 6.1, and we refer to this traversal pattern, always prioritzing traversal of horizontal (or vertical) edges that do not pass through the boundary of the fundamental polygon, as a *snake*. Repeated applications of the symmetries described above can transform an edge of G to an edge of this hamilton cycle, so G is edge-hamiltonian.

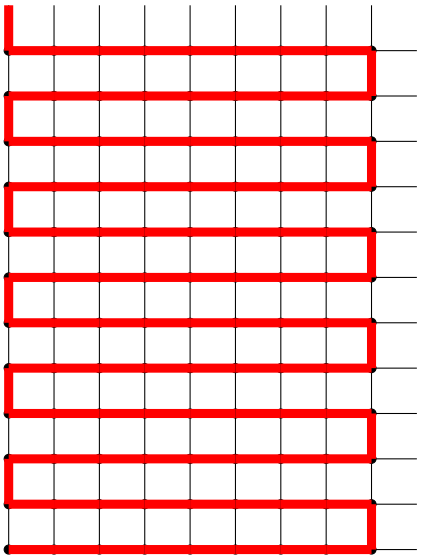

Figure 6.1. A hamilton cycle in $Q_g(12, 8)$.

If a black-black diagonal e_1 is added to one of the four-cycles of G, the resulting graph has no hamilton cycle through e_1. Since G has an even number of vertices and every edge of G has endvertices of opposite colors, a hamilton cycle containing e_1 would include a path on an odd number of edges of G with both endvertices black, contradicting the bipartiteness of G. The following proposition constitutes most of the proof of Theorem 6.1.

Proposition 6.3. *Let G be a bipartite member of the grid-type family $Q_g(p, r)$ of quadrangulations of the Klein bottle with partition sets of white and black vertices. If we add a black-black diagonal e_1 and a white-white diagonal e_2 in distinct quadrangles of G, then every edge of $G \cup \{e_1, e_2\}$ lies on a hamilton cycle.*

Proof. Without loss of generality, we may assume one endvertex of e_1 has coordinates $(1, 2j)$ for some $1 \leq j < p/2$, and we divide analysis of black-black edges into four cases $(1, 2j)$-$(1 \pm 1, 2j \pm 1)$. Similarly, we will consider white-white edges of four types: $(2k \pm 1, 2l \pm 1)$-$(2k, 2l)$. We will first describe how to begin hamilton cycles using each e_1 type, then describe how to finish each with a white-white edge

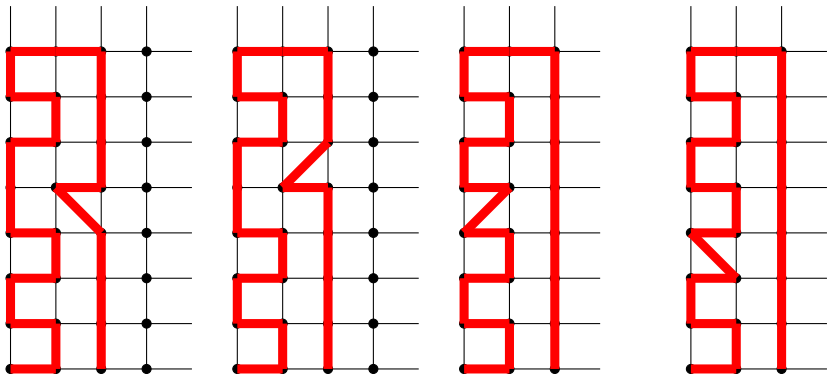

Figure 6.2. Representatives of each family of black-black edges. The bottom-left vertex is at $(0, 0)$.

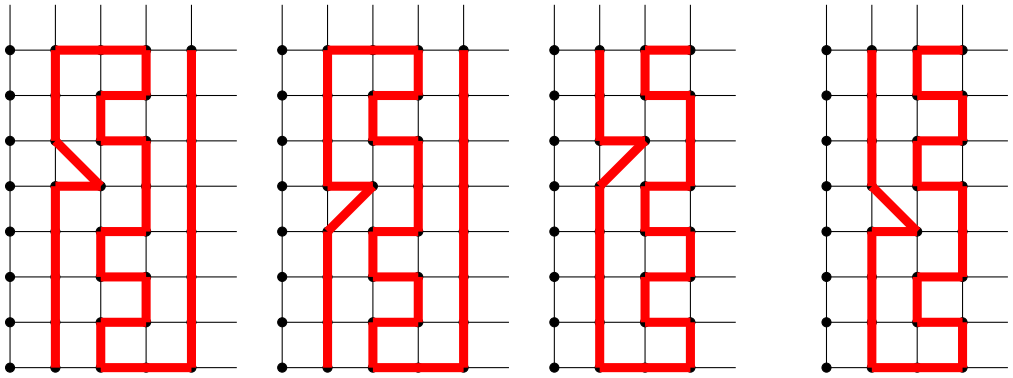

Figure 6.3. Representatives of each family of white-white edges with r even. The top-right vertex is at $(r, p-1)$.

e_2, addressing most possibilities with these general instructions. Finally we will analyze the few outlying pairs of diagonal edges.

We begin a hamilton cycle as shown in Figure 6.2; we will refer to the path through the first two columns, restricting to edges with both endvertices on a pair of vertical lines, as a *sawtooth*. In most cases there is a natural continuation to any of the e_2 types, shown in Figure 6.3 if both endvertices of e_2 are farther right in the grid than the right endvertex of e_1.

For $i \in \{0, 1\}$ if e_1 has endvertices $(i, 2j + i + 1)$ and $(i + 1, 2j + i + 1 \pm 1)$ for some $0 \leq j \leq \frac{p}{2} - 1$ and e_2 has endvertices $(2k, 2l)$ and $(2k \pm 1, 2l \pm 1)$ with $k > 1$ and $0 \leq l \leq \frac{p}{2} - 1$, a sequence of vertical paths snaking to connect the examples given completes a hamilton cycle through e_1 and e_2. The only remaining cases that

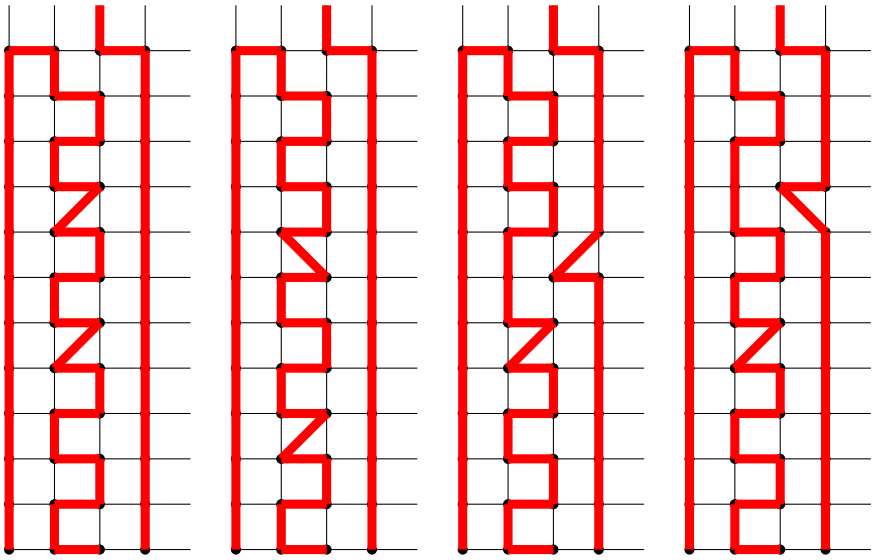

Figure 6.4. Beginnings of hamilton cycles with e_1 and e_2 near each other.

require special consideration are those in which at least one endvertex of e_1 is in the same column as an endvertex of e_2. Again invoking the symmetries of G, we may assume without loss of generality that the lower endvertex of e_2 is not lower than the lower endvertex of e_1.

We consider the four remaining cases in two groups with $i \in \{0, 1\}$. First, if e_1 has endvertices $(i, 2j + i + 1)$ and $(i + 1, 2j + i + 1 \pm 1)$ for $0 \leq j \leq \frac{p}{2} - 1$ and e_2 has endvertices $(i, 2k + i)$ and $(i + 1, 2k + i \pm 1)$ we consider two cases: both e_1 and e_2 have higher (or lower) right endvertex or one diagonal has a higher right endvertex and the other lower. Second, if e_1 has endvertices $(i, 2j + i + 1)$ and $(i + 1, 2j + i + 1 \pm 1)$ and the left endvertex of e_2 has x-coordinate $i + 1$, then we consider two analogous cases. If the x-coordinates of the endvertices of e_1 and e_2 are the same, the hamilton cycle sawtooths through two consecutive p-cycles as shown in the first two graphs in Figure 6.4. If the endvertices of e_1 share exactly one x-coordinate with the endvertices of e_2, the hamilton cycle sawtooths through two consecutive p-cycles as shown in the second two graphs of Figure 6.4, bypassing one endvertex of e_2 through which it detours as it traverses the next p-cycle. □

Finally, we use this proposition to prove Theorem 6.1, which we restate here.

Theorem 6.1. *Let G be a bipartite grid-type quadrangulation of the Klein bottle with partition sets of white and black vertices. If we add a nonempty set E_1 of one or more black-black diagonals to the quadrangles of G, then no element of E_1 lies on a hamilton cycle in $G \cup E_1$. However, if we add one further white-white diagonal e_2 in a quadrangle of $G \cup E_1$, then each edge of $G \cup E_1 \cup \{e_2\}$ lies on a hamilton cycle of that graph.*

Proof. We first observe that no edge of E_1 can be in a hamilton cycle of $G \cup E_1$, for every other edge of this graph has at least one black endvertex. If $e_1 = xy$, then we would need to find a hamilton path between x and y in $G \cup E_1 \backslash e_1$. Such a path has an odd number of edges and passes through two more white vertices than black, so at least one edge of the path would need both endvertices white, and there is no such edge. Let e be an edge of $G' = G \cup E_1 \cup \{e_2\}$. If $e \in E(G)$, then the edge-hamiltonicity of G implies e is included in a hamilton cycle of G'. If $e \in E_1$, then Proposition 6.3 describes how to find a hamilton cycle of G' through e and e_2. Similarly, if $e = e_2$, then Proposition 6.3 describes how to find a hamilton cycle of G' through e and some $e_1 \in E_1$. □

6.3 Ladder-type Quadrangulations

As with grid-type quadrangulations, we follow the notation given in [23] to define the family $Q_l(2p, r)$ of 4-regular quadrangulations of the Klein bottle. To construct a graph in this family, place vertices at integer points in the plane from $(0, 0)$ to $(r, 2p)$ and add all edges along line segments from $(i, 0)$ to $(i, 2p)$ for $\leq i \leq r$ and line segments from $(0, j)$ to (r, j) for $0 \leq j \leq 2p - 1$. Finally, identify $(i, 0)$ with $(i, 2p)$ for $0 \leq i \leq r$ and add edges $(0, j)$-$(0, j + p)$ and (r, j)-$(r, j + p)$ for $0 \leq j \leq p - 1$. After this identification, all calculations involving y-coordinates

will be done modulo $2p$; for visual reference, consider the fundamental polygon of the Klein bottle a neighborhood bounding $[0, r] \times [0, 2p - 1]$.

Graphs in this family are grids on cylinders capped with Möbius ladders, and it is easy to see they are bipartite exactly when p is odd. We shall refer to vertices by the coordinates (x, y) given in the initial construction and in the bipartite case color a vertex white if its coordinates are congruent modulo 2 and black otherwise.

It is straightforward to verify edge-hamiltonicity of graphs in $Q_l(2p, r)$; since examples are very similar to the hamilton cycles for edges of grid-type quadrangulations we omit this discussion. We shall exploit various symmetries of ladder-type quadrangulations in proving the results of this section, especially the rotational symmetry of the cylinder. As with the grid-type graphs, we begin with a pair of diagonals in distinct quadrangles.

Proposition 6.4. *Let G be a bipartite member of the ladder-type family $Q_l(2p, r)$ of quadrangulations of the Klein bottle with partition sets of white and black vertices. If we add a black-black diagonal e_1 and a white-white diagonal e_2 in distinct quadrangles of G, then each edge of $G \cup \{e_1, e_2\}$ lies on a hamilton cycle.*

Proof. We separate the proof into four cases, depending on whether one or both of e_1 and e_2 are in quadrangles of a Möbius ladder and whether they are in the same Möbius ladder. For simplicity, we omit unused edges of Möbius ladders in the caps of the cylinder in the figures accompanying this proof.

Case 1. *Both e_1 and e_2 are diagonals of grid quadrangles.*

We may assume without loss of generality that the endvertices of e_1 have y-coordinates 0 and 1 and that the left endvertex of e_2 has x-coordinate at least that of the left endvertex of e_1. To see the first, we observe two automorphisms of G. A decrease of all y-coordinates by a multiple of 2 or an increase of y-coordinates so

e_1's endvertices have y-coordinates $2p-2$ and $2p-1$ followed by $y \to 2p-1-y$ is a color-preserving isomorphism of $Q_l(2p, r)$ that maps the endvertices of e_1 to vertices with y-coordinates 0 and 1. To see the second, observe that decreasing all y-coordinates of vertices of G by one maintains the relative horizontal positions of e_1 and e_2 while switching their colors.

Given that e_1 has endvertices with y-coordinates 0 and 1, we consider four subcases.

Case 1.1. *The y-coordinates of the endvertices of e_1 and e_2 are the same.*

As we have already argued, we may assume both e_1 and e_2 have endvertices with y-coordinates 0 and 1 and that the x-coordinate of at least one of e_1's endvertices is less than both those of e_2. In this case, we describe a hamilton cycle starting at $(0, 0)$ as shown in Figure 6.5. Rungs of the Möbius ladder cylinder caps are not included. Starting at $(0, 0)$, traverse edges to unvisited vertices, avoiding rungs of the Möbius ladders, following edges that change y-coordinate between 0 and 1 whenever possible, and increasing x-coordinate by one otherwise. This will "sawtooth" through the vertices with y-coordinates 0 and 1, traversing e_1 and e_2, and end at $(r, 1)$ if r is even or at $(r, 0)$ if r is odd.

If r is even, follow the path along vertices on $x = r$ to $(r, 2p-1)$, then to $(r-1, 2p-1)$ and down to $(r-1, 2)$ and continue this pattern "snaking" through the rest of the grid. If r is odd, follow a similar snaking pattern, but start with the edge $(r, 0)$-$(r, p-1)$. In both cases, this will complete a hamilton path at $(0, 2p-1)$; since this vertex is adjacent to $(0, 0)$ we have a hamilton cycle.

Case 1.2. *The x-coordinates of the endvertices of e_1 and e_2 are the same.*

Let i and $i+1$ be the x-coordinates of the endvertices of e_1 and e_2; if e_2 has an endvertex with y-coordinate $2p-1$, increase all y-coordinates by 2 so neither

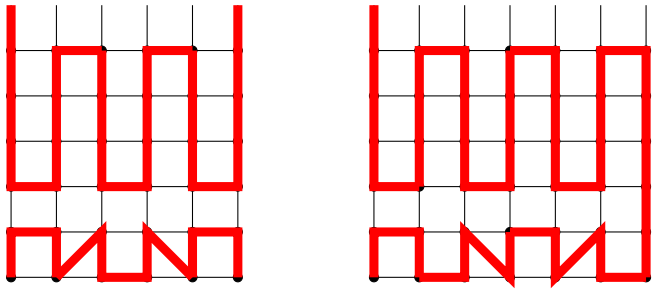

Figure 6.5. Case 1.1: Both e_1 and e_2 have endvertices with y-coordinates 0 and 1.

endvertex of e_2 has y-coordinate $2p-1$. If this is done, e_1 will no longer have endvertices with y-coordinates 0 and 1; the following description of a hamilton cycle requires only that neither e_1 nor e_2 have an endvertex with y-coordinate $2p-1$. Sawtooth, starting along $y=0$, through columns i and $i+1$ to $y=2p-2$. If i is even, stop at $(i+1, 2p-2)$; if i is odd, stop at $(i, 2p-2)$. Continuing to avoid the vertices with y-coordinate $2p-1$, snake to the end of column 0 or r, depending the parity of i. This path will visit all vertices of the boundary column except the one with y-coordinate $2p-1$ and terminate in an adjacent vertex. Carry out the same process on the other side of the column, starting at the bottom, add the edges $(0,0)$-$(0,2p-1)$ and $(r,0)$-$(r,2p-1)$, and include all edges on the line $y=2p-1$. Examples are shown in Figure 6.6, from which rungs of the Möbius ladder cylinder caps are omitted.

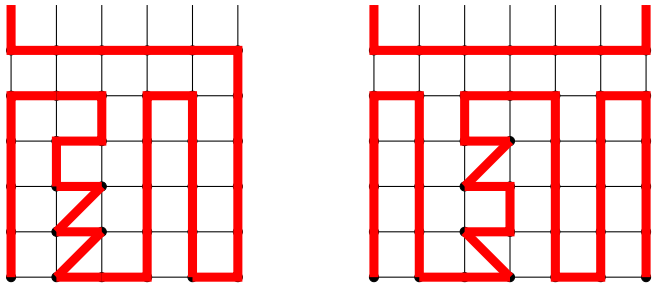

Figure 6.6. Case 1.2: The endvertices of e_1 and e_2 share the same x-coordinates.

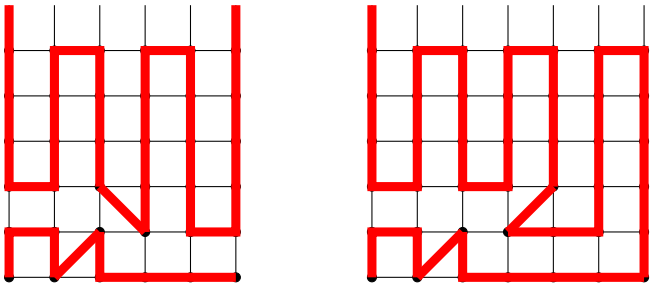

Figure 6.7. Case 1.3: Endvertices of e_1 and e_2 share one y-coordinate.

Case 1.3. *The endvertices of e_2 have y-coordinates 1 and 2.*

Let the endvertices of e_2 have coordinates $(j, 1)$ and $(j+1, 2)$ (rising) or $(j, 2)$ and $(j+1, 1)$ (falling). The symmetry of the graph implies we may assume at least one endvertex of e_1 has x-coordinate less than j. Examples of hamilton cycles described in the next paragraph are illustrated in Figure 6.7.

Begin a hamilton cycle at $(0, 0)$ and sawtooth along the bottom two rows until reaching a vertex below e_2. Then, moving to the bottom row if necessary, visit all remaining vertices with y-coordinate 0. Snake through all remaining vertices in the columns to the right of e_2 until reaching $(j+2, 1)$ if e_2 is rising or $(j+2, 2p-1)$ if e_2 is falling. Snake through the remaining vertices, traversing e_2, to $(0, 2p-1)$, which is adjacent to $(0, 0)$.

Case 1.4. *The endvertices of e_1 and e_2 have 4 different y-coordinates and at least 3 different x-coordinates.*

Start a hamilton cycle at $(0, 0)$ and sawtooth through the bottom two rows until reaching a vertex below e_2. Then, moving to the bottom row if necessary, visit all remaining vertices with y-coordinate 0. If e_2's left endvertex has even x-coordinate j, snake to the lowest unvisited vertex in column $j+2$ then sawtooth through columns j and $j+1$ to $(j, 2p-1)$. Finish by snaking to $(0, 2p-1)$- $(0, 0)$. If e_2's left endvertex has odd x-coordinate, snake to the highest unvisited vertex

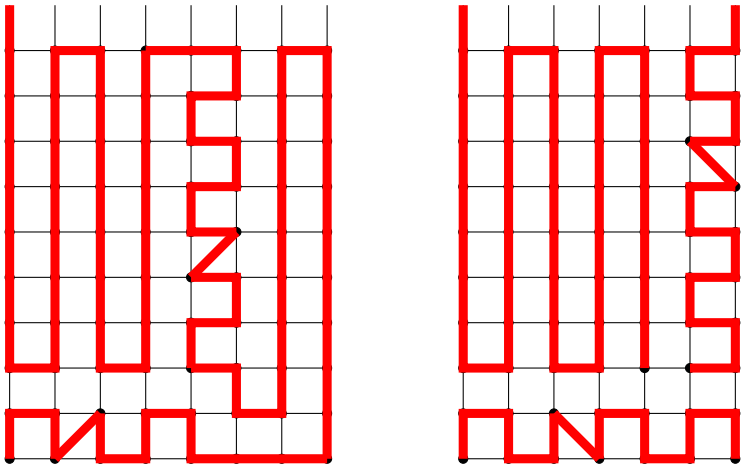

Figure 6.8. Case 1.4: e_1 and e_2 are far from each other.

in column $j+2$ then sawtooth through columns j and $j+1$ to $(j,2)$ and complete the hamilton cycle as before, as shown in Figure 6.8.

Case 2. *One diagonal is in a grid quadrangle and the other is in a Möbius ladder quadrangle.*

We may assume without loss of generality that e_1 has endvertices $(0,2p-1)$ and $(0,p-2)$. If both endvertices of e_2 have x-coordinate at least 2, start a hamilton cycle with $(0,0)$-$(0,2p-1)$, traverse e_1 and follow the path along the rim of the Möbius ladder to $(0,p+1)$. After traversing the rung of the Möbius ladder to $(0,1)$, begin a sawtooth with $(0,1)$-$(0,2)$ and end at $(1,p-1)$. Follow the path along vertices $(1,i)$ to $(1,p+2)$ then sawtooth to $(1,2p-1)$ as shown in Figure 6.9. Snake through all but the bottom two vertices of the remaining columns until reaching a column containing an endvertex of e_2. Unless e_2's endvertices have y-coordinates 1 and 2, sawtooth through this and the next column, then snake to column r. If e_2's endvertices have y-coordinates 1 and 2, these later columns will include vertices with y-coordinate 1. This path will reach $(r,2)$ with $(r,1)$ unvisited, $(r,2p-1)$, or $(r,1)$. The last situation will arise only when e_2 has endvertices with y-coordinates 1 and 2. In this case, follow the bottom row until under e_2. In

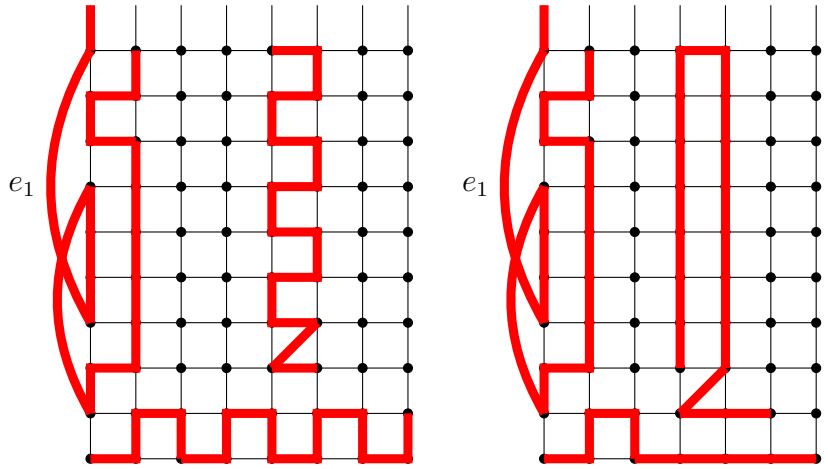

Figure 6.9. Case 2: Beginning, middle, and end of hamilton cycles.

all cases, sawtooth through the bottom two rows until finishing the hamilton cycle with $(1,1)$-$(1,0)$-$(0,0)$.

If e_2 has endvertices with x-coordinates 1 and 2, sawtooth columns 0, 1, and 2 below the diagonal and columns 2 and 3 above, as shown in Figure 6.10. If e_2 has endvertices with x-coordinates 0 and 1, we may assume without loss of generality that its endvertices have y-coordinates between $p-2$ and $2p-1$; otherwise the quadrangulation's symmetry implies we may consider e_1 having endvertices $(0, 2p-1)$ and $(0, p)$. Start a hamilton cycle at $(0,0)$, follow the path on vertices with x-coordinate 0 until one endvertex of e_1, traverse e_1, then sawtooth down columns 0 and 1, through e_2, until reaching $(1, p-1)$. Next, follow the path on vertices with x-coordinate 0 until $(1,1)$ and snake through the remaining columns, avoiding vertices with y-coordinate 0. When all vertices with y-coordinate greater than 0 have been visited, the path will terminate at a vertex adjacent to $(r,0)$. After following the edge to $(r,0)$, the remaining unvisited vertices lie on a path back to $(0,0)$ as shown in Figure 6.10.

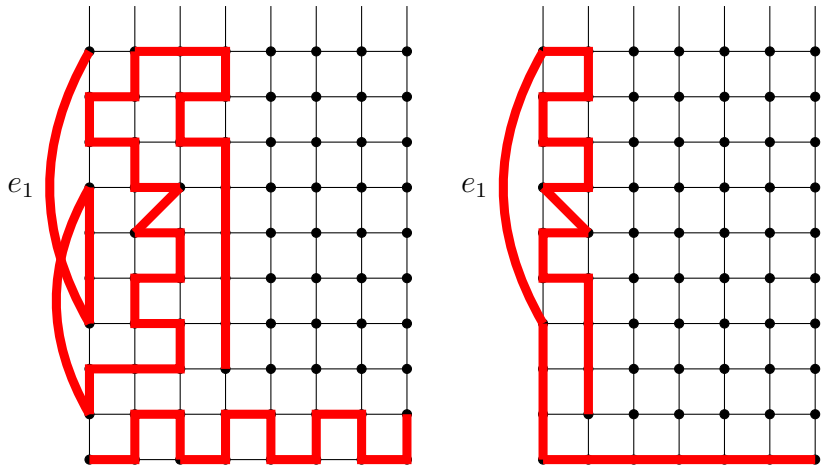

Figure 6.10. Case 2: Beginning and end of hamilton cycles with e_2 near the Möbius ladder.

Case 3. *Both diagonals are in quadrangles of the same Möbius ladder.*

Without loss of generality, assume both e_1 and e_2 are diagonals of the Möbius ladder all of whose vertices have x-coordinate 0. We describe a hamilton path for the vertices of this ladder from $(0,0)$ to $(0,1)$, assuming without loss of generality e_2 is the edge $(0,0)$-$(0,p+1)$. Starting at $(0,0)$, traverse edges of the Möbius ladder starting with $(0,0)$-$(0,p+1)$-$(0,p)$ and at each vertex $(0,i)$ choose an edge to continue to an unvisited vertex according to the following priority, where all y-coordinates are reduced modulo $2p$:

1. e_1
2. $(0,i)$-$(0,i+p)$
3. $(0,i)$-$(0,i-1)$

This path will visit all vertices with x-coordinate 0, starting at $(0,0)$ and ending at $(0,1)$. Continue a hamilton cycle through the entire graph by snaking through all vertices with y-coordinate not 0. Depending on the parity of r, this path will terminate at $(r,1)$ or $(r,2p-1)$, both of which are adjacent to $(r,0)$. Continue

to $(r, 0)$ and follow the path along the bottom row back to $(0, 0)$ to complete the hamilton cycle.

Case 4. *The diagonals e_1 and e_2 are diagonals of opposite Möbius ladders.*

In this (final) case, we assume without loss of generality e_1 has endvertices $(0, 2p-1)$ and $(0, p-2)$. Let (r, k) and $(r, k+p)$ be the endvertices of e_2; this implies r and k have the same parity. We begin with a path through all vertices of one Möbius ladder from $(0, 0)$ to $(0, 2)$, then give a path through all vertices of the other Möbius ladder and describe how to connect the two in a hamilton cycle. Starting at $(0, 0)$, choose an edge to traverse from $(0, i)$ to an unvisited vertex according to the following priority until reaching $(0, p+3)$:

1. e_1
2. $(0, i)$-$(0, i+p)$
3. $(0, i)$-$(0, i-1)$

Finish this path with $(0, p+3)$-$(0, p+2)$-$(0, p+1)$-$(0, 1)$-$(0, 2)$.

We consider paths through all vertices with x-coordinate r according to the parity of r, first addressing odd r. After discussing the completion of hamilton cycles joining vertices in opposite ends of the grid, we describe how to adapt this discussion for r even.

If r is odd, most choices of e_2 can be traversed in a path through all vertices with x-coordinate r, starting at $(r, 0)$ and ending with $(r, p+3)$-$(r, p+2)$-$(r, p+1)$-$(r, 1)$-$(r, 2)$. Starting at $(r, 0)$, choose an edge to traverse from (r, i) to an unvisited vertex according to the following priority, where all calculations are module $2p$, until reaching $(r, p+3)$:

1. e_2

2. (r, i)-$(r, i + p)$

3. (r, i)-$(r, i - 1)$

The specific choices of e_2 not addressed by this general description are those with at least one endpoint $(r, p + 2)$ or $(r, 1)$. For each such e_2, the deviations from the above process are small, and we describe them below.

If $e_2 = (r, 1)$-$(r, p + 2)$, start with $(r, 0)$-$(r, 1)$-$(r, p + 2)$-$(r, p + 1)$ and traverse edges following the above priorities through all vertices with x-coordinate r and terminating at $(r, 2)$.

If $e_2 = (r, 1)$-(r, p), start with $(r, 0)$-$(r, 2p - 1)$, then follow the above priorities until reaching $(r, p + 2)$; finish with $(r, p + 2)$-$(r, p + 1)$-(r, p)-$(r, 1)$-$(r, 2)$.

If $e_2 = (r, 3)$-$(r, p + 2)$, follow the above priorities until traversing e_2, then finish with $(r, p + 2)$-$(r, p + 1)$-$(r, 1)$-$(r, 2)$.

We have given paths through all vertices with x-coordinate 0 and through all vertices with x-coordinate r both having endvertices with y-coordinates 0 and 2. Connect these paths with a sawtooth through the bottom two rows and snake vertically through the other rows, as shown in Figure 6.11.

If r is even, increase all y-coordinates by 1 (modulo $2p$) in the path through vertices with x-coordinate r. These paths will now be between $(r, 1)$ and $(r, 3)$. Extending to $(r, 1)$-$(r - 1, 1)$-$(r - 2, 2)$ and $(r, 3)$-$(r - 1, 3)$-$(r - 1, 4)$ and continuing to snake to $(r - 1, 2p - 1)$ then to $(r - 1, 0)$ we may complete a hamilton cycle as described for r odd.

This final case completes our proof of Proposition 6.4. □

This proposition is the bulk of the work needed to prove Theorem 6.2, which we restate here.

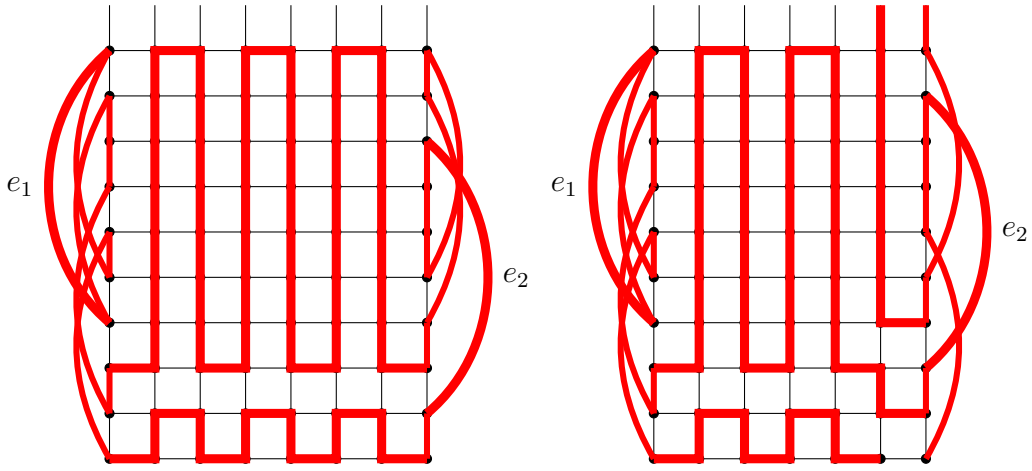

Figure 6.11. Case 4: The diagonals are in quadrangles of opposite Möbius ladders.

Theorem 6.2. *Let G be a bipartite ladder-type quadrangulation of the Klein bottle with partition sets of white and black vertices. If we add a nonempty set E_1 of one or more black-black diagonals to the quadrangles of G, then no element of E_1 lies on a hamilton cycle in $G \cup E_1$. However, if we add one further white-white diagonal e_2 in a quadrangle of $G \cup E_1$, then each edge of $G \cup E_1 \cup \{e_2\}$ lies on a hamilton cycle of that graph.*

Proof. Since each edge of $G \cup E_1 \cup \{e_2\}$ is an edge of G or a black-black diagonal or a white-white diagonal, the proof is the same as the proof of Theorem 6.1, using Proposition 6.4 instead of Proposition 6.3. □

6.4 Mesh-type Quadrangulations

Our main results are about bipartite grid-type and ladder-type quadrangulations of the Klein bottle. There is a third family of 4-regular quadrangulations. Mesh-type quadrangulations $Q_m(p, r)$ can be constructed by placing vertices at integer points (x, y) of the plane where $0 \leq x \leq r$, $0 \leq y \leq 2p$, and $x \equiv y (\text{mod } 2)$. Edges in these graphs are between (x, y) and $(x \pm 1, y \pm 1)$. To quadrangulate the Klein bottle, identify vertices at $(2i, 0)$ with $(2i, 2p)$ for $0 \leq i \leq r/2$ and identify vertices at $(0, 2j)$ with $(r, 2p - 2j - [r \mod 2])$ for $0 \leq j \leq p$.

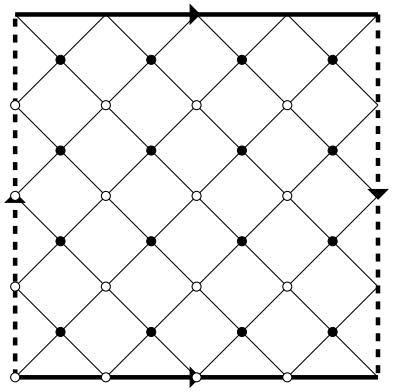

Figure 6.12. A bipartite mesh-type quadrangulation of the Klein bottle.

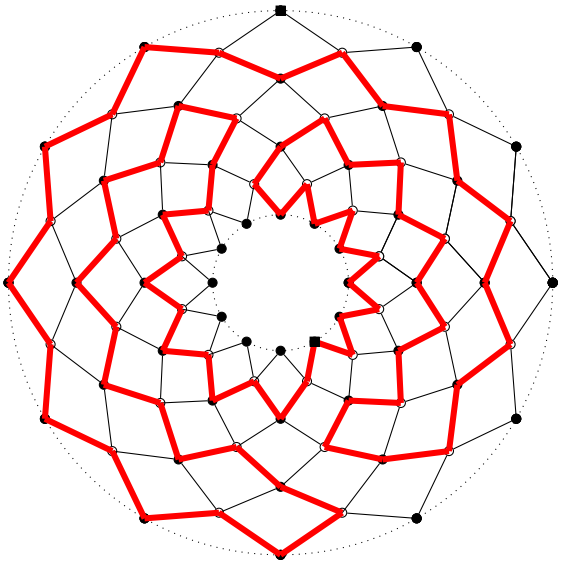

Figure 6.13. A hamilton cycle in a mesh-type quadrangulation.

Mesh-type quadrangulations $Q_m(p,r)$ are bipartite precisely when r is even; the color classes are determined by parity of y-coordinate. Without loss of generality we say white vertices have even y-coordinates. We describe a hamilton cycle in $Q_m(p,r)$ below and note the the complement of the edge set of this hamilton cycle is another hamilton cycle in $Q_m(p,r)$. It follows that $Q_m(p,r)$ is edge-hamiltonian. Beginning at $(0,0)$ travel from a white vertex $(2i,2j)$ to $(2i+1,2j+1)$. From a black vertex $(2i+1,2j+1)$ travel to $(2i,2j+2)$ if this vertex is unvisited; otherwise travel to $(2i+2,0)$. This (hamilton) path will terminate at $(r-1,2p-1)$, which is adjacent to $(0,0)$ across an unused edge. Traverse this edge to complete the hamilton cycle. Since $Q_m(p,r)$ has an equal number of white and black vertices, the addition of a black-black diagonal to a quadrangle of the graph destroys edge-hamiltonicity. It is more tedious, however, to verify that addition of a white-white edge introduces a hamilton cycle that includes the black-black edge. In the grid-type and ladder-type quadrangulations we were able to show edge-hamiltonicity by grouping many black-black or white-white edges into single cases; we did not need to consider separately each pair of equivalence classes of their endpoints.

We illustrate edge-hamiltonicity of a mesh-type quadrangulation in Figure 6.13. The outer dotted circle is identified with the inner dotted circle with opposite orientations, and one pair of identified vertices is marked with squares. Observe that the complement of the edges in the hamilton cyle indicated by thick red edges is also a hamilton cycle.

Chapter 7
Conclusion

In this chapter we review our results and consider future work in extending them. We also present a conjecture about the relationship between crossing number and genus of 2-amalgamations.

7.1 2-Crossing-Critical Graphs

In Chapters 2-4 we showed how to extend a family of 2-crossing-critical graphs on the plane to 2-crossing-critical graphs on surfaces of higher genus, both orientable and non-orientable. In particular, the set $\mathcal{T}(\mathcal{S})$ consists of twisted tile belts whose general structure is like a Möbius ladder, as tiles alternate in sequence between inverted and not-inverted until the last tile, which is joined to the first tile after a half-twist. We defined the family $\mathcal{T}^+(\mathcal{S})$, each member of which is obtained from a graph in $\mathcal{T}(\mathcal{S})$ by avoiding the half-twist of the last tile in sequence and adding a not-inverted tile to the end of the sequence before identifying the right boundary vertices of the last tile with the left boundary vertices of the first tile. The resulting tile belt has two rim cycles, which we call *inside* and *outside*. We add a hub vertex adjacent to three inside rim vertices and three outside rim vertices. We showed graphs in the set $\mathcal{T}^+(\mathcal{S})$ are 2-crossing-critical on the projective plane, regardless of which six tiles contain the six neighbors of the hub.

For $\mathbb{N}_g$ the non-orientable surface of genus $g \geq 1$, we showed graphs in $\mathcal{T}_g(\mathcal{S})$, each of which is the union of one graph in $\mathcal{T}^+(\mathcal{S})$ and $g-1$ graphs in $\mathcal{T}(\mathcal{S})$, are 2-crossing-critical on $\mathbb{N}_g$. The construction of graphs that are 2-crossing-critical on $\mathbb{N}_g$ came at the cost of connectivity; each member of $\mathcal{T}^+(\mathcal{S})$ is 3-connected while for $g \geq 2$ no member of $\mathcal{T}_g(\mathcal{S})$ is connected; each has $g-1$ components, each of which is 3-connected. The authors of [2] constructed twisted tile belts to characterize 2-crossing-critical graphs that contain a Möbius ladder topological minor. As V_6

is a forbidden topological minor for embedding in the plane, results on graphs containing a V_8 minor helped guide this inquiry. All the graphs H_t defined in [16] and all the graphs in $\mathcal{T}^+(\mathcal{S})$ have a V_{10} topological minor. As embeddings in both orientable and non-orientable surfaces of positive genus are less well understood than embeddings in the plane and the list of forbidden topological minors for the projective plane contains 103 graphs and is unknown for other surfaces, it seems unlikely all 2-crossing-critical graphs for the projective plane with a V_{10} topological minor are in one of these families. To continue this work, we plan to follow the broader approach taken in [2] to characterize 2-crossing-critical graphs on the projective plane that do not have a V_8 minor. The list of forbidden topological minors should inform this search.

For surfaces of higher genus the lists of 1-crossing-critical graphs are not known. This implies that the characterizations of 2-crossing-critical graphs are much farther off than a characterization for even the projective plane, but it would be informative to find a set of 3-connected, 2-crossing-critical graphs for an orientable surface of genus at least one or non-orientable surface of genus at least two. For orientable surfaces, we have defined a set of 2-crossing-critical graphs with a number of 2-separations equal to the genus of the surface. We are examining branching twisted tile belt structures to see whether it is possible to find a structure similar to the twisted tile belts for the plane that is consistent with the addition of handles to an orientable surface.

7.2 Crossing Numbers and Genus

In [6], the authors give a result that allows computation of the (orientable) genus of a 2-amalgamation of two graphs. We use this result and the absence of an alternating genus embedding of a graph to exercise some control over the genus and crossings of a 2-amalgamation. While additivity of genus and additivity of

crossing number over amalgamations are active areas of study, we are interested in combining the two. In particular, we offer the following conjecture.

Conjecture 7.1. *Let G be a graph with orientable genus $k \geq 1$ and crossing number s on $\mathbb{S}_{k-1}$, and let H be a graph with orientable genus $l \geq 1$ and crossing number t on $\mathbb{S}_{l-1}$. Suppose G has a pair of vertices x_G, y_G such that G has no x_G, y_G-alternating embedding in $\mathbb{S}_k$ and H has a pair of vertices x_H, y_H such that H has no x_H, y_H-alternating embedding. Let $G \underset{\{x,y\}}{\cup} H$ be the 2-amalgamation of G and H obtained by identifying x_G with x_H and y_G with y_H. The orientable genus of $G \underset{\{x,y\}}{\cup} H$ is $k + l$ and the crossing number of $G \underset{\{x,y\}}{\cup} H$ on $\mathbb{S}_{k+l-1}$ is the smaller of s and t.*

If true, this conjecture would be a powerful tool in generating 2-crossing-critical graphs for orientable surfaces of arbitrary genus by amalgamating 2-crossing-critical graphs on surfaces of lower genus.

7.3 Hamiltonicity of 4-connected Graphs on the Klein Bottle

While proofs of the conjectures of Grünbaum and Nash-Williams remain elusive, we provide some progress toward understanding edge-hamiltonicity of 4-connected graphs on the Klein bottle. Edge-hamiltonicity is a stronger property than hamiltonicity, but as Ellingham and Marshall suggest for the torus a suitable modification may be to prove that every 2-connected graph on the Klein bottle has a Tutte cycle through any boundary edge, except if the graph contains a particular modification to certain bipartite families. The results presented here echo their torus result in illustrating the criticality of certain counterexamples to edge-hamiltonicity on the Klein bottle.

Initial progress toward proving hamiltonicity of 4-connected graphs on the torus and Klein bottle concerned 5-connected graphs. More general topological results

require higher connectivity, since there are non-hamiltonian 4-connected graphs embeddable in surfaces of negative Euler genus.

There are also quadrangulations of the Klein bottle that are not 4-connected, but can have their connectivity increased by addition of edges inside some faces. These quadrangulations are not as symmetric as the 4-regular types, so determining counterexamples to edge-hamiltonicity and their criticality requires many more cases to be examined. However, an understanding of how to recover a hamilton cycle after a domino transformation on two consecutive quadrangles may help in this regard. We observe that grid-type quadrangulations of the Klein bottle may be converted to ladder-type quadrangulations by consecutive domino transformations. Given that known counterexamples to edge-hamiltonicity on the Klein bottle, as on the torus, are critical in the sense we have described, we have some evidence that bipartiteness is an essential property of counterexamples to edge-hamiltonicity on the Klein bottle.

References

[1] D. Bokal. Infinite Families of Crossing-critical Graphs With Prescribed Average Degree and Crossing Number. *J. Graph Theory* **65**:139-162, 2010.

[2] D. Bokal, B. Oporowski, R. B. Richter, and G. Salazar. Characterizing 2-crossing-critical Graphs. *Advances in Applied Mathematics*, **74**:23-208, 2016.

[3] R. Brunet, A. Nakamoto, and S. Negami. Every 5-connected Triangulation of the Klein Bottle is Hamiltonian. *Yokohama Math. J.* **47**:239-244, 1999

[4] R. Brunet and R.B. Richter. Hamiltonicity of 5-connected Toroidal Triangulations. *J. Graph Theory* **20**:267-286, 1995

[5] N. Chiba and T. Nishizeki. A Theorem on Paths in Planar Graphs. *J. Graph Theory* **10**:449-450, 1986

[6] Decker, R.W., Glover, H.H., and Huneke, J.P. Computing the Genus of the 2-Amalgamations of Graphs. *Combinatorica* 5:271-282, 1985

[7] R. Diestel, *Graph Theory, Fifth Edition*. Springer-Verlag, Heidelberg, Graduate Texts in Mathematics, Volume 173, 2016

[8] M.N. Ellingham and E. Marshall. Criticality of Counterexamples to Toroidal Edge-Hamiltonicity. *Graphs and Combinatorics* **32**:111-121, 2016

[9] M.R. Garey and D.S. Johnson, Crossing Number is NP-Complete. SIAM J. Alg. Disc. Meth. **4**:312-316, 1983

[10] Glover, H. H., Huneke, J. P., and Wang, C. S. 103 Graphs That Are Irreducible For the Projective Plane. *J. Combin. Theory Ser. B* **27**:332-370, 1979.

[11] R.J. Gould, Updating the Hamiltonian Problem - A Survey. *J. Graph. Theory* **15**:121-157, 1991

[12] R.J. Gould, Advances on the Hamiltonian Problem - A Survey. *Graphs and Combinatorics* **19**:7-52, 2003

[13] R.J. Gould, Recent Advances on the Hamiltonian Problem: Survey III. *Graphs and Combinatorics* **30**:1-46, 2014

[14] B. Grünbaum. Polytopes, Graphs, and Complexes. *Bull. Amer. Math. Soc.* **76**:1131-1201, 1994

[15] M. Hirsch, *Differential Topology*, 1976.

[16] P. Hliněný and G. Salazar. Stars and Bonds in Crossing-Critical Graphs. *Electronic Notes in Discrete Mathematics*, **8**:271-275, 2008.

[17] R.M. Karp, Reducibility Among Combinatorial Problems, in *Complexity of Computer Computations*. Plenum, New York, 1972

[18] K. Kawarabayashi, A Survey on Hamiltonian Cycles. *Interdiscip. Inf. Sci.* **7**:25-39, 2001

[19] B. Mohar, A Linear Time Algorithm for Embedding Graphs in an Arbitrary Surface. *SIAM J. Discrete Math.* **12**:6-26, 1999

[20] B. Mohar and C. Thomassen, *Graphs on Surfaces*. Johns Hopkins University Press, Baltimore, Johns Hopkins Studies in the Mathematical Sciences, Volume 10, 2001

[21] W. Myrvold and J. Roth. Simpler Projective Plane Embedding. *Ars Combinatoria*, **75**:135-155, 2005.

[22] W. Myrvold and J. Woodcock. A Large Set of Torus Obstructions and How They Were Discovered. *Electronic J. Comb.* **25**:P1.16, 2018.

[23] A. Nakamoto and S. Negami. Full-symmetric Embeddings of Graphs on Closed Surfaces. *Mem. Osaka Kyoiku Univ. Ser. III* **49**:1-15, 2000

[24] C. St. J. A. Nash-Williams. Unexplored and Semi-explored Territories in Graph Theory, in *New Directions in the Theory of Graphs*: 149-186, 1973

[25] B. Pinontoan and R.B. Richter. Crossing Number of Sequences of Graphs I: General Tiles. *Australas. J. Combin.* **30**:197-206, 2004.

[26] B. Pinontoan and R.B. Richter. Crossing Number of Sequences of Graphs II: Planar Tiles. *J. Graph Theory* **4**:332-341, 2003.

[27] R.B. Richter and G. Salazar, Crossing Numbers, in *Selected Topics in Topological Graph Theory*. Oxford University Press, 2009

[28] S. Stahl and L. W. Beineke. Blocks and the Nonorientable Genus of Graphs. *J. Graph Theory* **1**:75-78, 1977.

[29] R. Thomas and X. Yu. 4-connected Projective-planar Graphs are Hamiltonian. *J. Combin. Theory Ser. B* **62**:114-132, 1994

[30] R. Thomas and X. Yu. 5-connected Toroidal Graphs are Hamiltonian. *J. Combin. Theory Ser. B* **69**:79-96, 1997

[31] R. Thomas, X. Yu, and W. Zang. Hamilton Paths in Toroidal Graphs. *J. Combin. Theory Ser. B* **94**:214-236, 2005

[32] C. Thomassen. A Theorem on Paths in Planar Graphs. *J. Graph Theory* **7**:169-176, 1983

[33] C. Thomassen. Tilings Of the Torus and Klein Bottle and Vertex-transitive Graphs On a Fixed Surface. *Trans. Amer. Math. Soc.* **323**:605-635, 19

[34] C. Thomassen, The Graph Genus Problem is NP-Complete. *J. Algorithms* **10**:568-576, 1989

[35] W.T. Tutte. A Theorem on Planar Graphs. *Trans. Amer. Math. Soc.* **82**:99-116, 1956

[36] W.T. Tutte. Bridges and Hamiltonian Circuits in Planar Graphs. *Aequationes Math.* **15**:1-33, 1977

[37] R. P. Vitray, The 2 and 3 Representative Projective Planar Embeddings. *J. Combin. Theory Ser. B*, **51**:1-12, 1992.

[38] H. Whitney. A Theorem on Graphs. *Ann. Math.* **32**:378-380, 1931

Vita

Joshua E. Fallon was born in West Palm Beach, Florida. He finished his undergraduate studies at Palm Beach Atlantic University in May 2004. He earned a Master of Science degree in Mathematical Sciences from Florida Atlantic University in May 2007. In August 2013 he came to Louisiana State University to continue graduate studies in mathematics. He is currently a candidate for the degree of Doctor of Philosophy in mathematics.